1969

A study of simulated boiling in vertical upward and downward flow

Chandrakant V. Mahale
Lehigh University

A STUDY OF SIMULATED BOILING IN VERTICAL UPWARD AND DOWNWARD FLOW

by

Chandrakant V. Mahale

A THESIS

Presented to the Graduate Committee

of Lehigh University

in Candidacy for the Degree of

Master of Science

in

Mechanical Engineering

Lehigh University

1969

To my Professors

CERTIFICATE OF APPROVAL

This thesis is accepted and approved in partial fulfillment of the requirements for the degree of Master of Science.

April 21 1969
(date)

Alan H Stenning
Professor in Charge

Ferdinand P. Beer
Head of the Department

ACKNOWLEDGEMENTS

I wish to thank Professor Alan H. Stenning for his kind guidance and most helpful suggestions during the course of this work.

I am grateful to Professor Thomas E. Jackson and Professor J. V. D. Eppes for their help in photography.

I thank Mr. Frank J. Pechacek Jr. for his help in some of the modifications of the test rig. and Dr. Lawrence P. Golan for his help and suggestions.

The financial support provided by the Esso Research and Engineering Company, Florham Park, New Jersey is deeply appreciated.

ACKNOWLEDGEMENTS

I wish to thank Professor Alan H. Stenning for his kind guidance and most helpful suggestions during the course of this work.

I am grateful to Professor Thomas E. Jackson and Professor J. V. D. Eppes for their help in photography.

I thank Mr. Frank J. Pechacek Jr. for his help in some of the modifications of the test rig. and Dr. Lawrence P. Golan for his help and suggestions.

The financial support provided by the Esso Research and Engineering Company, Florham Park, New Jersey is deeply appreciated.

TABLE OF CONTENTS

LIST OF FIGURES

NOMENCLATURE

D	Diameter
L	Length
R	Radius
$\bar{r}$	Distance of probe aperture from the centre of the pipe.
F.V.P.	Full view photograph of the flow pattern
A.B.	Air boiled in cft/min.
W	Water flow rate in gallons/min.
C.V.P.	Close view photograph of the flow pattern just after the boiling area
A.I.	Air introduced in the up flow
o	Water rate of 5 gpm and different air rates
□	Water rate of 10 gpm and different air rates
△	Water rate of 15 gpm and different air rates.
T	Temperature in ^{o}F
P1, P2, P3, P4, P'	PSIG (pressure gauges)
V1	Valve
V	Velocity
P	Probing
B	Boiling

A STUDY OF SIMULATED BOILING IN VERTICAL UPWARD AND DOWNWARD FLOW

by

Chandrakant V. Mahale

ABSTRACT

An investigation of the distribution of air and water in the upflow tube, U-bend and downflow tube of a two phase flow apparatus is presented here with the help of experimental results and photographs.

Isokinetic and sampling probes were used to sample the flow. Probing was done at the centres and at the beginning of the upflow and downflow tubes.

The visual observations of flow patterns in the downflow tube are illustrated with the help of photographs.

It can be concluded that poor heat transfer at low liquid flow rates may be partly due to the presence of vapour cavities in the U-bend and in the downflow tube. Higher liquid flow rates eliminated the vapour cavities.

I. INTRODUCTION

1.1 General

Two-phase flows, both with and without boiling, occur in many industrial situations. Circular tubes are the cheapest of the possible geometric configurations and in consequence horizontal and vertical arrangements of circular tubes, connected by U-bends, are frequently employed. Although a great deal of research has been carried out on two-phase fluid behavior and heat transfer in horizontal flow and vertical upflow, relatively little has been done on vertical downflow.

1.2 Previous Work

L. Pujol [1] found that at low vapor quality, there was a distant difference between the boiling heat transfer coefficients in upflow and downflow, with substantially higher heat transfer coefficients occurring in the upflow legs of his apparatus. In addition, he observed that in general the boiling heat transfer coefficients on the outer radius of the U-bends were higher than those on the inner radius.

This effect was particularly severe in the bottom U-bends, for which gravity and centrifugal effects combined to move the liquid away from the inner radius.

L. P. Golan [2] studied flow patterns, void fractions, and pressure drop characteristics of two-phase air-water mixtures in vertical pipes connected by U-bends. He found that the dominant downflow pattern was one with a central core of vapor surrounded by an annular film of liquid on the wall of the tube. This observation suggested that the downflow tube should be well coated with liquid, and appeared to contradict Pujol's observation of low heat transfer in the downflow tubes. However, when Golan simulated boiling by injecting air bubbles into the liquid, he discovered a new phenomenon. In the upflow tube, the air broke away from the wall and moved upward as separate bubbles. In the downflow tube, the air tended to form a large vapor cavity below the injection point, and to cling to the wall. Evidently the flow pattern associated with boiling was quite different from that obtained with a mixture of constant proportions, and a vapor blanket at the wall could be responsible for the observed heat transfer behavior.

The objective of the present study was to extend Golan's work by injecting air into the water through a section of porous bronze tubing, thus simulating boiling, and to observe the resulting flow patterns and phase distributions in the straight legs and the upper U-bend.

II. EXPERIMENTAL EQUIPMENT AND OPERATING PROCEDURE

2.1 General

The goal of this investigation was to study flow patterns in upflow, U-bend, and downflow tubes at low air-water rates with air injection. The experimental equipment constructed by Golan was used for this study. The two phase flow facility, a semiclosed loop, is shown schematically in Fig. 1(b) while an overall photograph of the system is shown in Fig. 1(a). Four major sections of the flow system are as follows.

2.2 Water line

The distilled water used for the experiments was U.S.P. pure. Water was stored in a 55 gallon capacity stainless steel drum. One foot below the upper rim of the drum a stainless steel strainer was placed to avoid splashing of the water. It also served to screen foreign matter and eliminate air which might otherwise be carried to the water pump. Fig. 13 in Golan's dissertation shows the storage drum with the external splash shield in position.

The storage drum and water pump are connected by a 1-1/2 inch stainless steel pipe. A stainless steel ball valve located between the pump and storage drum was used to control the water supply from the storage drum. The water pump was an all bronze Worthington centrifugal pump type ICNF-52 with a bronze impeller. A drip proof induction motor of specifications: 5 hp, 60 cps, 3600 rpm, 220/440 volts was used to drive the pump. The pump characteristics were flat over the flow range used in the tests (3-20 gpm)- see Fig. 14 of [2].

The water flow was controlled by a 1-1/2 inch Jenkins globe valve with a Brooks rotameter model number FV-1110-10 size 13 being used to meter the flow rate. The range of this rotameter was 3.7 to 37 gpm of water. The rotameter float type was 13-RV-760, and the scale length was 250 mm direct reading in gpm of water with the calibrated accuracy of the instrument being 1% of full flow.

2.3 Air line

An Ingersoll-Rand class ER1 air compressor was used to supply the air. The maximum capacity of this compressor was 190 scfm at 100 psig. This air compressor fed air to a 200 cft surge tank which helped to smooth out the fluctuations in the air supply. A

Pall Corporation Ultipor air filter situated at the outlet of the surge tank removed particles greater than five microns in diameter.

The low air flow supply was pressure regulated by an Airco 806-9969 single stage pressure regulator. The capacity of this instrument is 30 cfm of free air at 45 psig. The flow rate through this regulator was controlled by a 1/4 inch Jenkins globe valve. Low air flows were measured on a Brooks rotameter FV type 1110-07 H2AIA. The capacity of this meter was 0-2.85 scfm of air at 70^{o}F and 60 psig. The calibrated accuracy of this instrument was 1% of full flow. The static pressure at the low air flow meter was measured by a Helicoid test gage of calibrated accuracy of 1%. The air temperature was measured by a 120^{o} mercury thermometer. Air could be mixed with water in a mixing tee before the test section, or injected into the test section through a porous bronze sleeve.

2.4 Test Section

Acrylic plastic tubes of 1-1/2 inch inside diameter and 1/4" thickness were used in the transparent part of this section. Figure 2 shows the schematic of the test section with approximate dimensions. The upflow riser height was 121.5" with a length to tube diameter ratio of 81. The downflow tube length was 109.5" with a length to tube diameter ratio of 73. Four pressure gages were used, two in up flow and two in downflow to measure the pressure drops in the respective tubes. The range of the pressure gages was 0-60 psi. The static pressure taps were 1/32" in diameter and were located approximately six inches before and after each U-bend. In the upflow tube the distance between the static pressure taps was 110" and in the downflow tube it was 97.5". The U-bends were machined from solid acrylic blocks to an inside diameter of 1-1/2" with a centre line to centre line spacing between up and downflow legs of 4-1/2" i.e., three tube diameters. The plastic tubes were flanged at the ends. 1/16" cork gaskets or neoprene gaskets were used between all flanged tubes to prevent leakages. Figure 2 shows the schematic diagram of the test section. Figure 4 (a-b-c-d) shows where the boiling and probing sections were installed for our investigations.

To simulate boiling a special piece was made. This piece was 10-1/2" in length with flanges at the ends. A porous bronze sleeve of 7" length was glued to two end-plastic pieces. An air chamber of 4" outside diameter and 7" long was made around the porous bronze sleeve. This whole piece is shown in Fig. 4(e).

During experiments air was supplied to the air chamber by a rubber hose and allowed to bubble through the sleeve and into the water flowing in the test section.

2.5 Sampling Equipment

Orange food dye was used (one ounce to 30 gallons of water) to colour the water.

Two types of probes were used for the phase distribution experimental portion of the investigation. The first was a probe designed to operate isokinetically, while the second was a simple sampling probe. These probes were used to obtain air-water samples from the main flow. The probing was done at three water flow rates of 5, 10, and 15 gpm at various quality levels. In all the graphs, the first number shows the water flow rate in gpm and the second number shows the air flow rate in scfm. The line diagram of the sampling equipment is shown in Figure 3 along with drawings of the isokinetic and sampling probes. A photograph of the probe positioner and the probe can be seen in Figure 22 of [2]. The isokinetic probe was constructed from a 0.125" pitot-static probe with the static measurement being performed inside the probe. The probe static pressure could be compared with the tube wall static pressure. When the static pressures were equal, isokinetic sampling was achieved. The static pressure taps on the tube wall sloped opposite to the flow direction in order to limit the water that entered the pressure lines. The sample flow line was relatively horizontal from the test section to the water measurement point.

The air-water separator was a centrifugal-gravity separator. The water was collected in a burette while the air-flow was measured by a precision Wet Test Flow Meter. The air flow meter could accurately measure flows down to 0.001 cft/hr. A water filled manometer was used to indicate the differential pressure between the sample probe and tube wall static pressure. At high water rates difficulty was experienced in trying to operate the probe isokinetically. The pressure lines filled with water and air slugs which fluctuated rapidly. For this reason after taking data for four different experimental setups (Fig. 4. a-b-c-d), the isokinetic probe was replaced by the sampling probe. Another reason for changing from the isokinetic probe to the sampling probe was that the isokinetic probe captured less than the correct amount of air. The same effect was experienced with the sampling probe but the effect was not as severe. For isokinetic probing, clamps located at the manometer inlet were used to damp the pressure fluctauations occurring to obtain a mean reading of the impact and static pressure.

The condition necessary to maintain isokinetic sampling was achieved by one of two means. Valve V1 (Fig. 3) would be opened to allow flow into the probe lines. As the valve was opened the static pressure in the tube would fall. The valve was opened until the probe and tube wall static pressures equalized. This condition indicated isokinetic sampling. During the minute of flow sampling the valve would be adjusted as necessary to maintain the equality of static pressures. If valve V1 could be fully opened without creating the equality of static pressures the vacuum pump would be started. By regulating the suction on the probe flow lines the probe static pressure could be lowered to the tube wall static pressure. During the minute of flow sampling the suction would be adjusted as necessary. All air-water flow lines in the probe system were 1/8 " O.D. tygon tubing. The sampling probe had a sampling area of 0.00138 square inches. The isokinetic probing was performed in the beginning and at the centre of the up-flow and downflow tubes, (as shown in

Fig. 4 a-b-c-d). The sampling probe was used at the beginning and at thecentre of the downflow tube, with valve V1 fully open.

2.6 Operating Procedure

First the compressor cooling water tap was opened. Once cooling water started circulating through the compressor cooling system, the compressor was started. The next step was to allow air into the porous bronze tube so that water was unable to enter the surrounding air chamber of the bronze sleeve. The water pump would be started and the water flow rate adjusted to the desired GPM level. The water rate was adjusted by a globe valve located just before the water flow meter. The air flow rate was controlled by a 1/4" globe valve on the low air flow supply. When air-water flows became stable sampling of the flow was done and also flow descriptions were noted down. Sampling of water flow rate in ml/min, air flow rate in cft/min, and pictures of the flow pattern completed the data necessary for one flow observation. The sampling was done across the tube cross section and fluid was collected for one minute at each sampling point.

III. TWO PHASE FLOW: COLOUR SLIDES

The investigation made here on flow patterns in vertical upward and downward two-phase flow was primarily a visual one. Many features of the flow occurred too quickly to be detected by the naked eye. To identify these features high speed colour slides were taken. The reasons for taking colour slides were:

1. We could project the slides on a screen and hence get a clear and enlarged picture of the phase distributions.
2. Colour slides could clearly distinguish the orange coloured water phase from the colourless air phase.

A Nikon F camera was used for taking the colour slides of the flow patterns. The shutter speed was one thousandth of a second. Four 500 watt bulbs supplied the necessary light. A gray card and a light meter were used to adjust the four bulbs to get a uniform brightness over the flow area of interest. Kodak high speed ektachrome colour film of type B was used to take slides. The light meter and gray card were useful in deciding aperture opening and speed of the shutter.

Figures 17 to 55 show black and white reproduction of the colour slides taken in this investigation. Figures 17 to 36 show the close-view and full-view flow patterns for an air rate of 2 scfm and water rates of 3-4-5-6-6.5-7-7.5-8-10-15 GPM. Figures 37 to 51 show the close-view and full-view flow patterns for an air rate of .25 scfm and water rates of 3-4-5-6-6.8-7-8-10-15 GPM. Figures 52 to 55 show the flow patterns with an initial air flow rate of 2 scfm (injected in tee section), air boiled through the sleeve equal to 2 scfm, and water rates of 3 GPM (Figures 52, 53, 54) and 1.5 GPM (Figure 55) respectively.

IV. EXPERIMENTAL OBSERVATIONS

The experimental study was divided into three main portions. First, measurements of the phase distributions were made in the upflow leg with air injected at the bottom of the upflow leg and the sampling probe located at the middle and the bottom of the upflow leg as shown in Figure 4(a) and 4(b). Next, phase distribution measurements were made in the downflow leg with air injected at the top of the downflow leg and the sampling probe located at the top and centre of the downflow leg as shown in Figure 4 (c) and 4(d). Finally, a photographic study of flow patterns in the upflow leg, upper U-bend and downflow leg was carried out. Simulated boiling numbers were of the order of 1×10^{-5} to 10×10^{-5} where the boiling number is defined as the ratio of the vapor mass production rate per unit surface area to the flow rate per unit cross section.

4.1 Phase Distribution in Upflow

Figure 5 shows the air distribution halfway up the upflow tube with air injected at the bottom of the upflow tube and Figure 6 shows the corresponding water distribution. Figures 7 and 8 show the air and water distribution at the bottom of the upflow tube. For each curve, the first number denotes the total water flow rate in gpm and the second number denotes the total air flow rate in standard cfm.

In studying the phase distribution plots, it is essential to realize that the sampling probe errors were so large that no reliance can be placed on the absolute magnitudes. However, at a given water flow rate and air flow rate, the shape of the curves probably gives a good indication of relative distribution.

The plots show that the air mixes with the water almost immediately in the up flow tube and there is no concentration of either phase on the wall or in the centre of the tube.

4.2 Phase Distribution in Down Flow

Figure 9 and 10 show the air and water distribution at the top of the down flow tube, with air injected just above the sampling section. At a water flow rate of 5 gpm, considerable asymmetry in phase distribution is observed, with the air flowing principally on one side of the tube, and the water flowing mainly on the other side. The significance of this phenomenon will become more apparent when the photographs are discussed.

At the higher flow rates of 10 and 15 gpm., the air is fairly well dispersed and the water has a higher flow rate at the centre of the tube than at the walls. Figures 11 and 12 show the phase distributions halfway down the tube. Some asymmetry is still observable at the lowest water flow rate, but at the higher water flow rates the flow pattern is approaching the annular flow observed by Golan, with the air mainly flowing in the central portion of the tube, and the water flowing in a film along the walls. Figures 13 and 16 give additional data confirming the earlier results.

4.3 Visual Observations of Flow in the Upper U-bend

The asymmetry noted in the down flow tube for a water flow rate of 5 gpm was also apparent to the naked eye, and a series of photographs were taken to follow the transition from asymmetric to symmetric flow in the upper portion of the tube. At low water flow rates, some air is able to rise above the injection zone and lodge in the U-bend, forming a cavity which extends from the U-bend into the down flow tube. As the water flow rate increases, the cavity shrinks in size until it disappears abruptly at a water flow rate of 7 gpm.

Figures 17 to 36 show this sequence of events for an air injection rate of 2.0 cfm and increasing water flow rates. At 7 gpm the flow below the injection zone changes from asymmetric cavity flow to froth flow. For an air flow rate of 0.25 cfm, the cavity behavior is essentially the same, except that after the cavity vanishes at / gpm the flow in the tube is bubbly. These flow patterns are shown in Figures 37 to 51.

Additional photographs were taken of cavities occurring when air was injected into a two-phase mixture of air and water created by mixing air in the tee section. Figures 52 to 55 show that the cavity is also present when the water approaching the U-bend contains some vapor. In these figures the initial air flow rate is 2 scfm, the injected air flow rate is 2 scfm, and the water flow rates are 3 gpm and 1.5 gpm.

For both the high and low air injection rates, the cavity disappears at a water flow rate of 7 gpm. This corresponds to a water velocity of 1.27 fps. The actual fluid mechanics of the phenomenon are extremely complex, involving gravity, shear and momentum effects. However, a rough estimate of the transition velocity can be made by assuming that the primary effect is a balance between gravity and centrifugal acceleration. Gravity tends to pull the liquid down from the top wall of the U-bend, while centrifugal acceleration tends to throw it upwards. Transition should occur approximately where these two effects are in balance i.e. when $\frac{V^2}{R} = g$.

With an outer U-bend radius of three inches, this gives a transition velocity of 2.8 fps. Above this velocity the liquid should be attached to the upper wall, while below it a cavity is possible. This value of velocity is roughly double the true transition velocity. It would be interesting to find out whether the transition velocity is in fact proportional to the square root of U-bend radius for U-bends with a ratio of tube diameter to outer U-bend radius different than that tested here.

V. CONCLUSIONS AND RECOMMENDATIONS

With vapor injection in the up flow tube, excellent mixing between the phases occurs and the vapor is distributed uniformly across the tube.

With vapor injection in the down flow tube, two interesting phenomena have been observed which may have some bearing on boiling heat transfer. At low liquid flow rates, a vapor cavity forms in the upper U-bend and persists over a substantial portion of the down flow tube. At higher liquid flow rates, the cavity disappears but in the region immediately after the vapor injection zone the liquid is forced away from the walls, and the annular configuration observed by Golan does not occur until the flow has been able to recover from the disturbance produced by vapor injection.

Additional experiments should be carried out with different tube and U-bend radii to obtain scaling laws for the transition from the cavity flow to well-mixed flow. In addition, it is desirable to carry out boiling experiments with conducting glass tubes so that the flow pattern actually occurring in down flow with boiling can be observed.

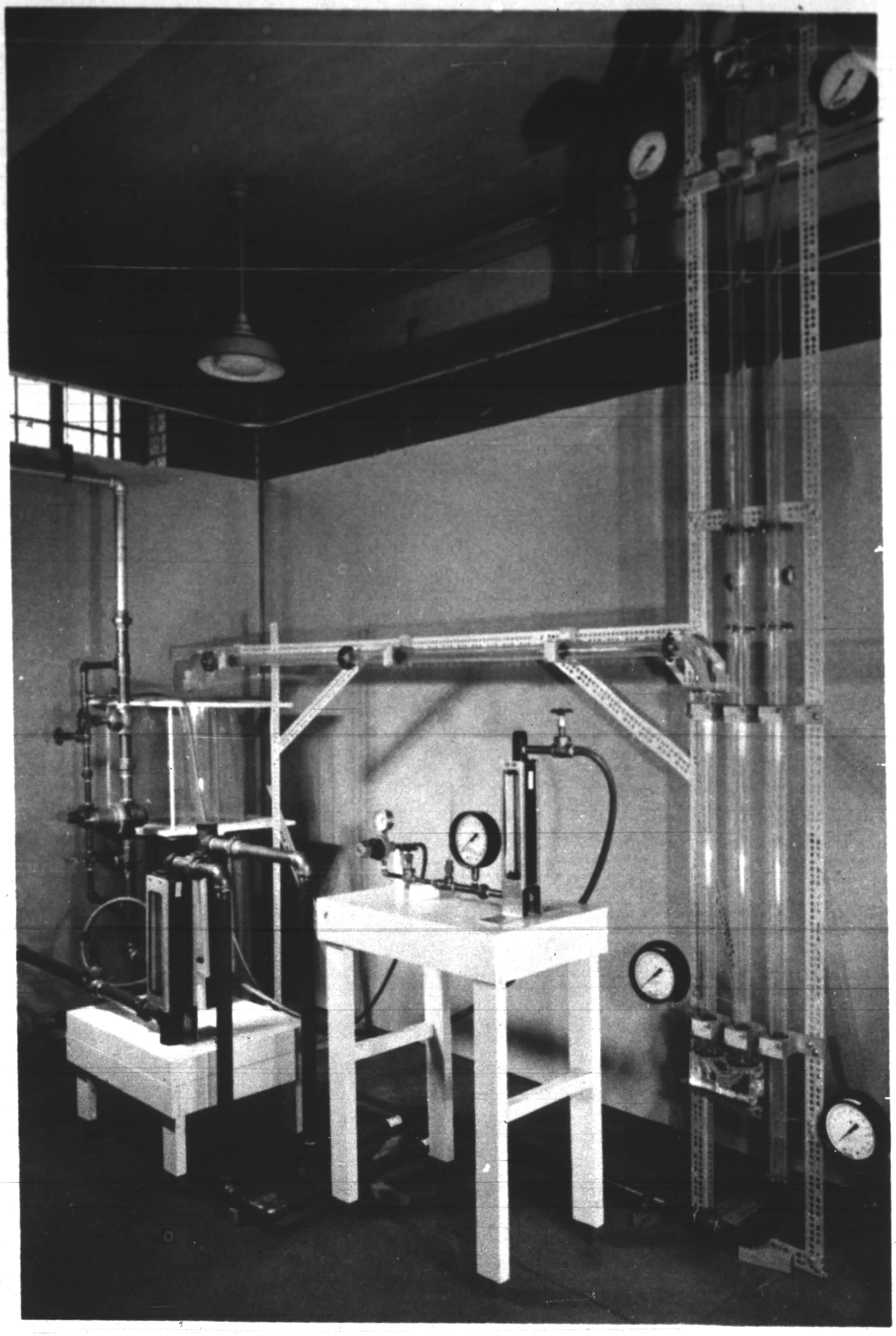

Photograph of the Two-Phase Flow Facility

Fig. 1(a).

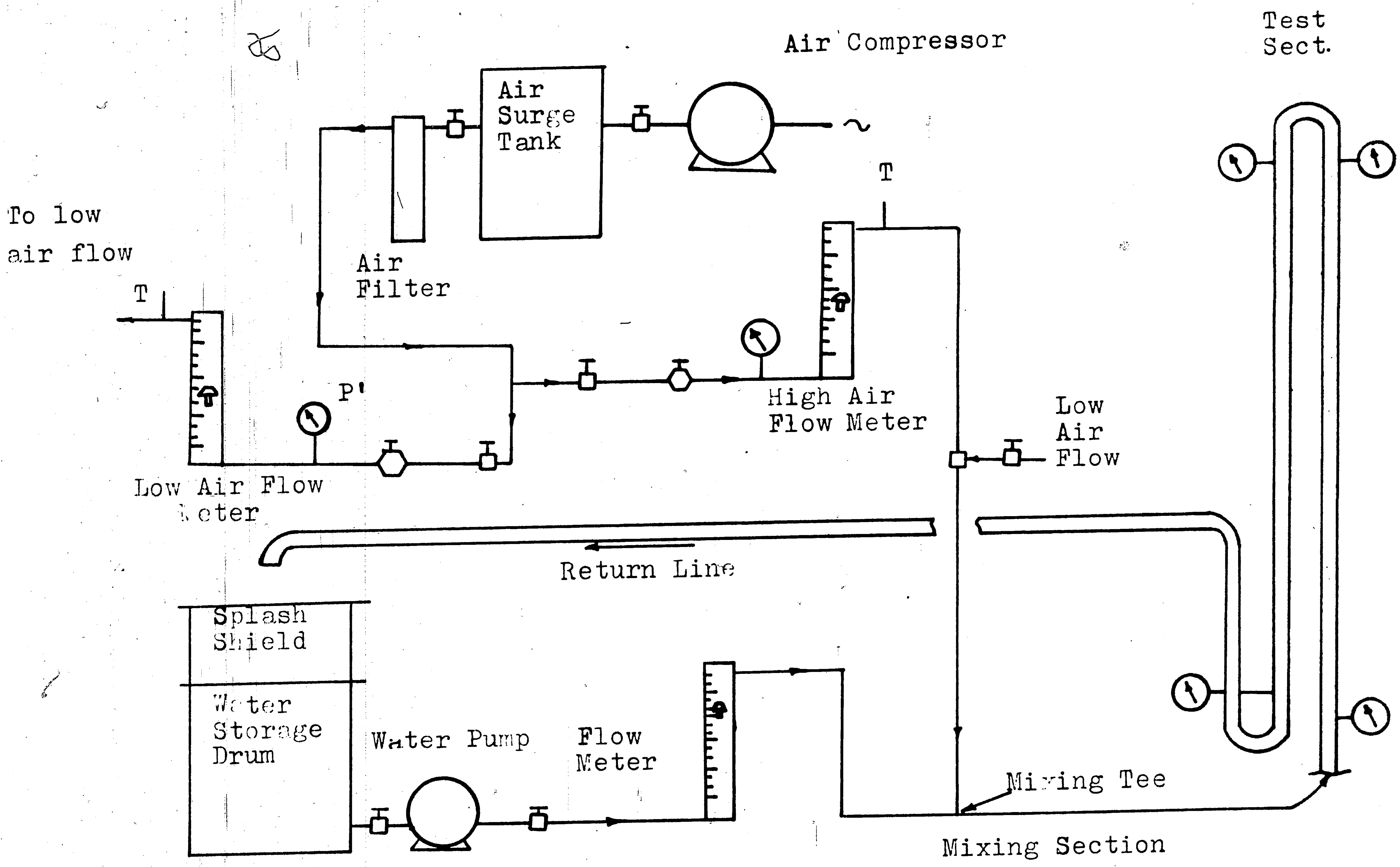

Schematic Diagram Of Flow System

Fig.1(b)

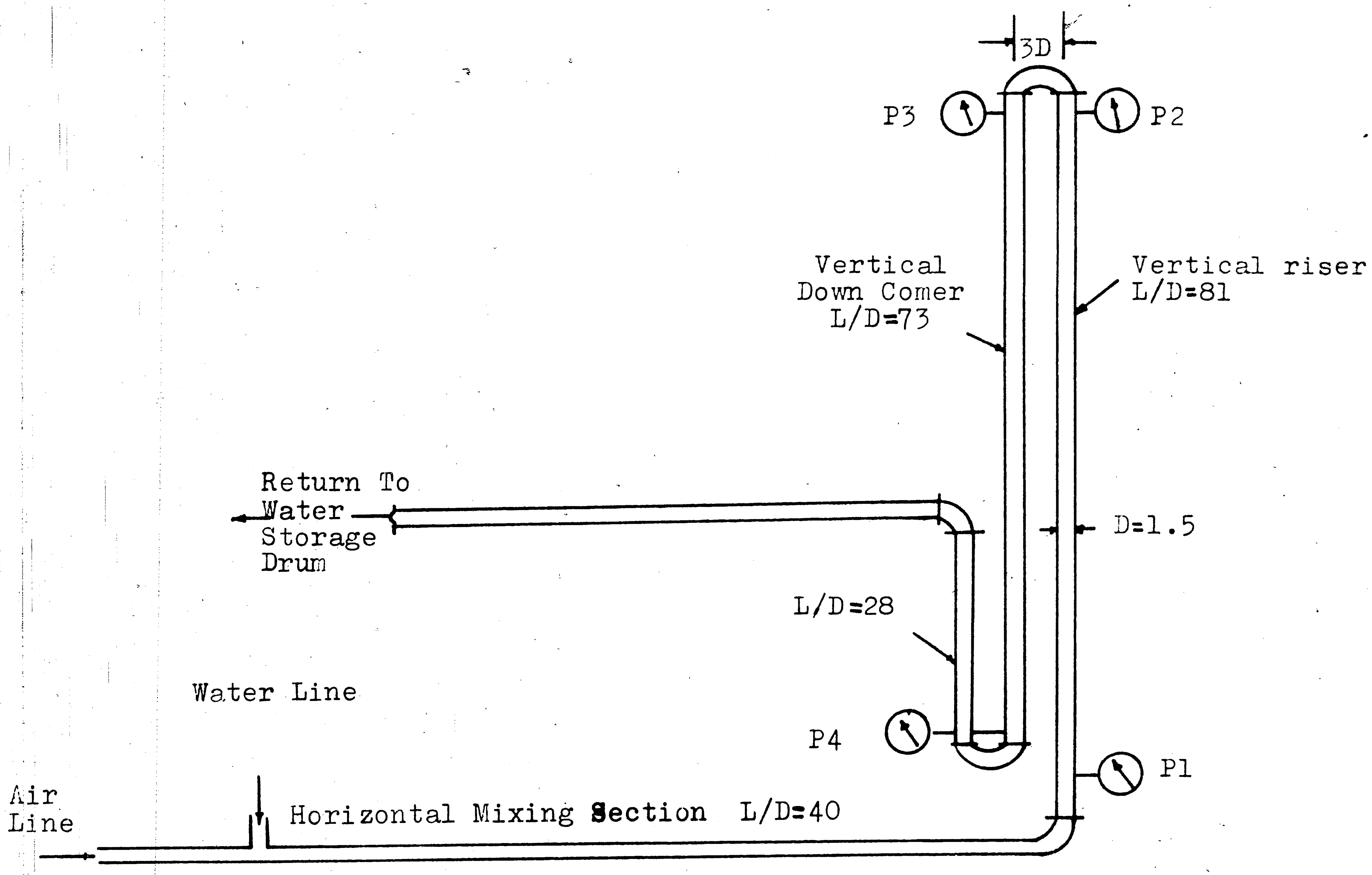

A Schematic Diagram of the Test Section
Fig.2.

The Isokinetic Sampling Instrument

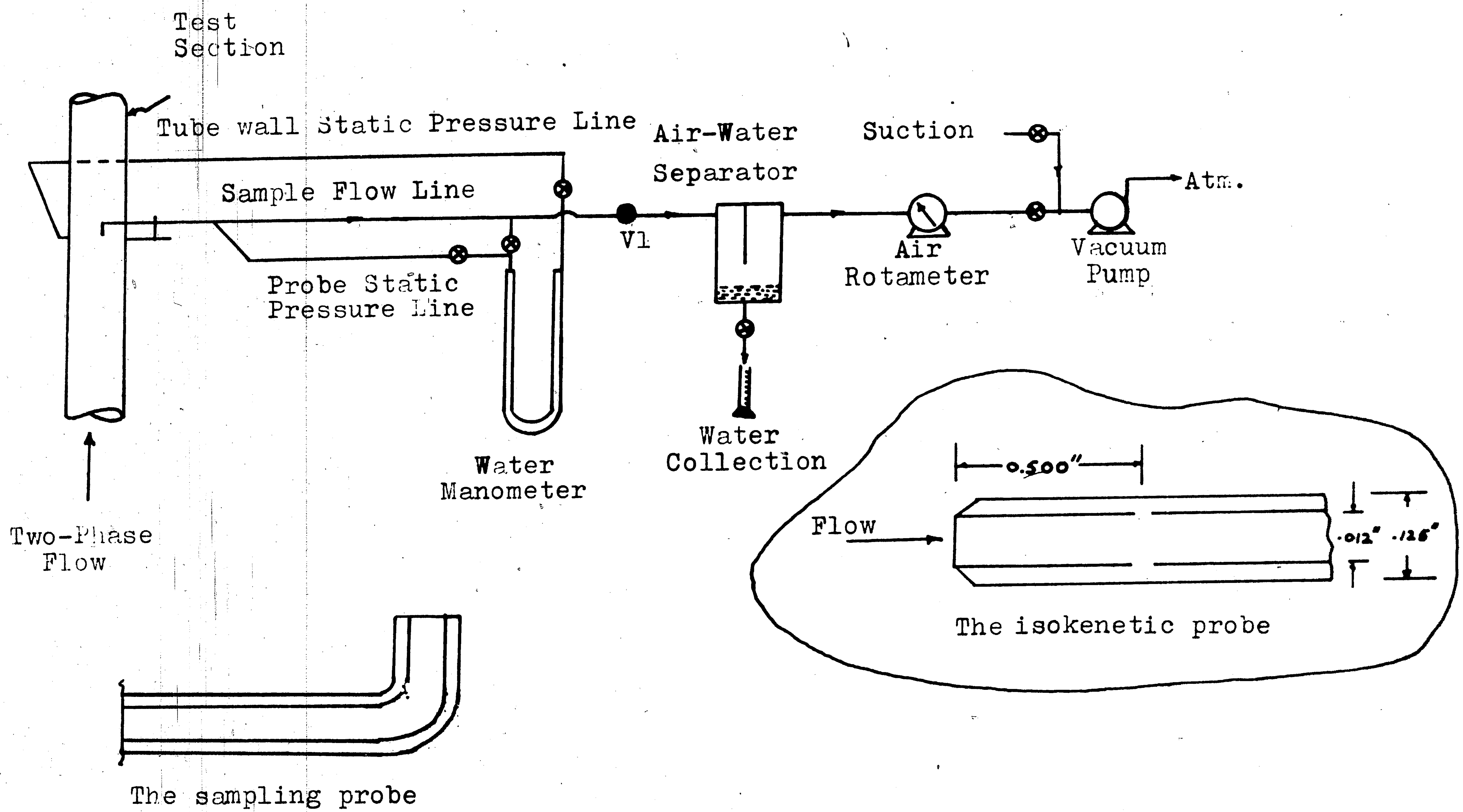

Fig.3.

Schematic diagrams showing different experimental set-ups of the test section

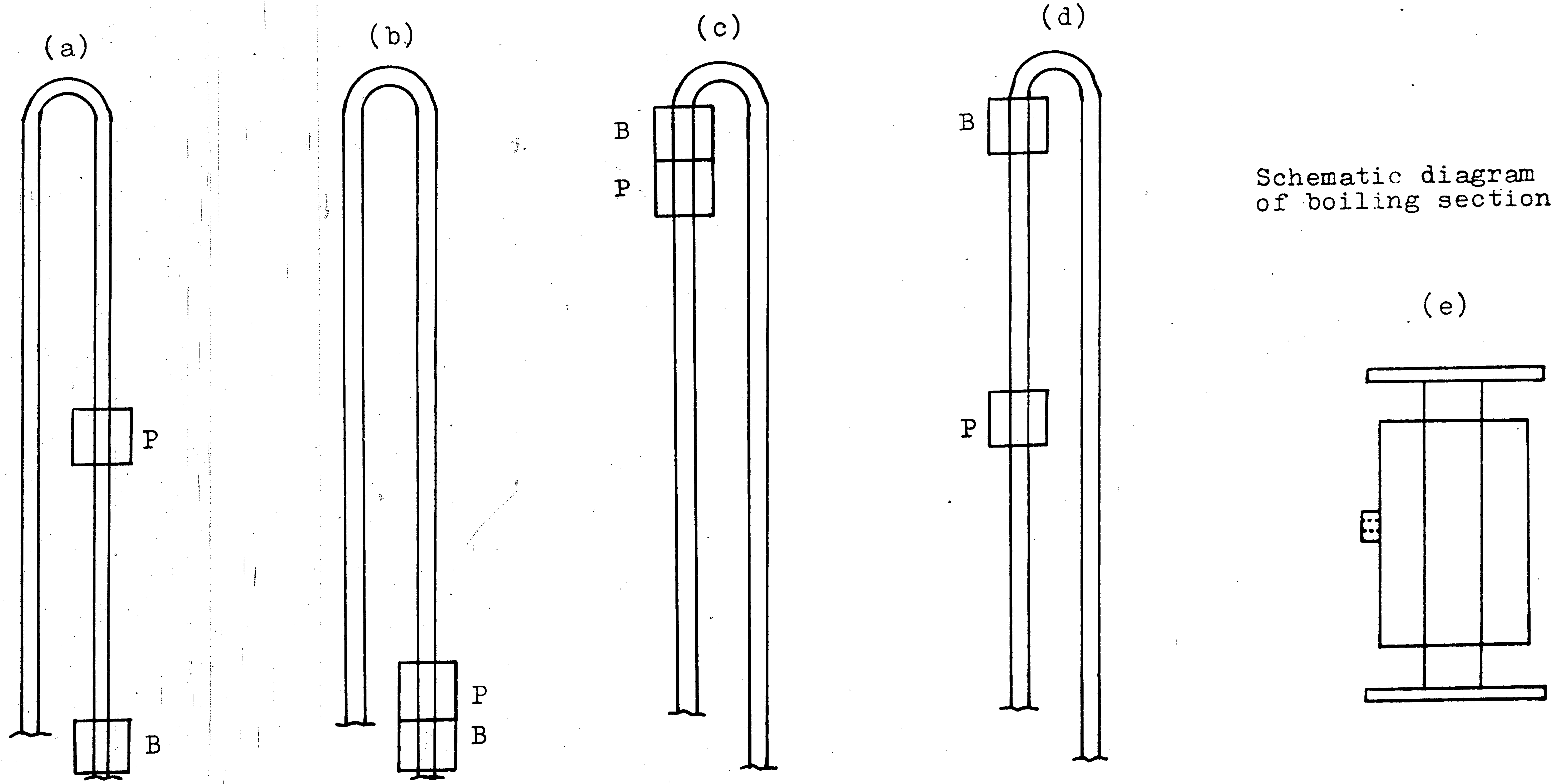

Fig.4.

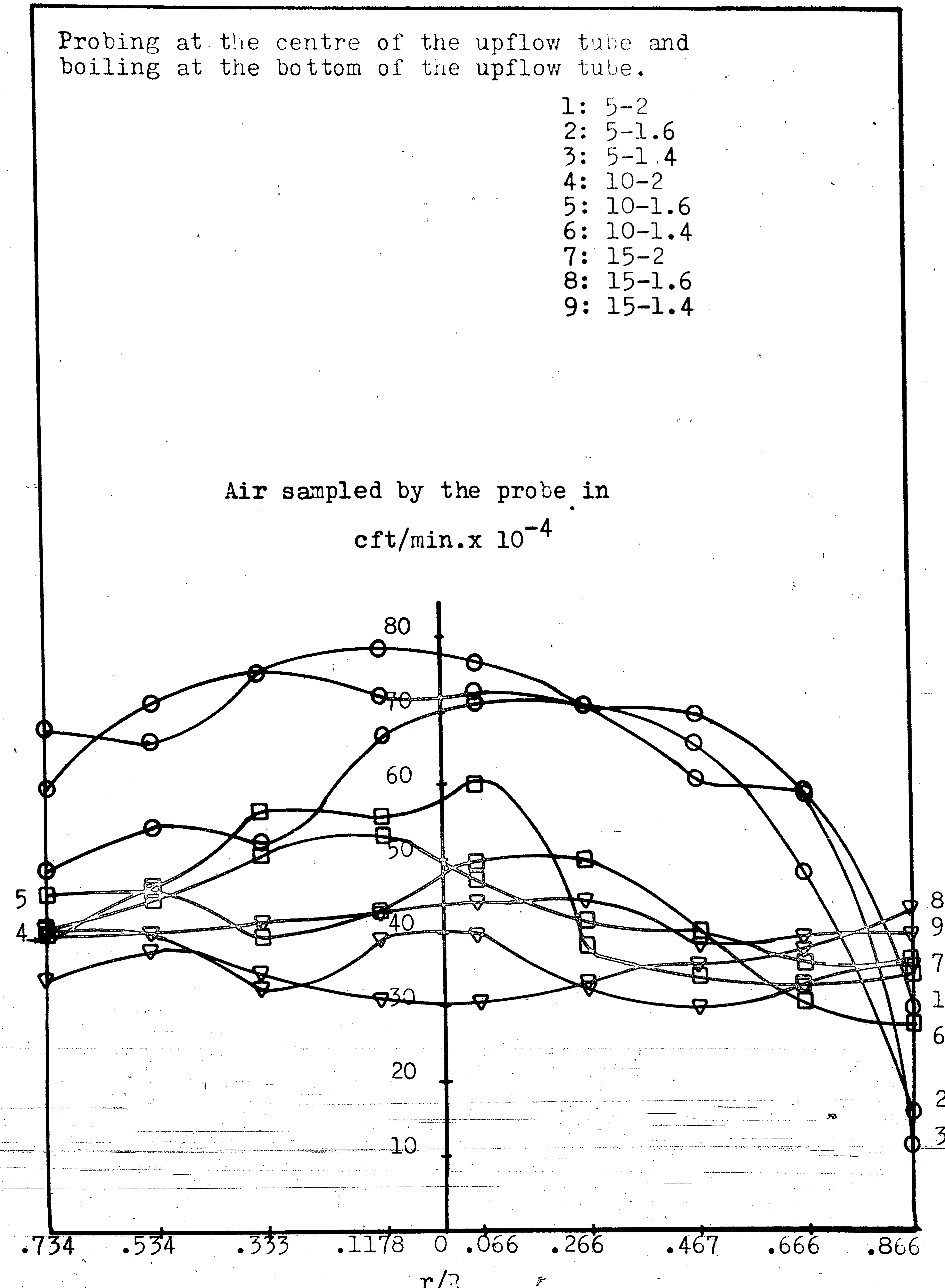

Probing at the centre of the upflow tube and
boiling at the bottom of the upflow tube.
1: 5-2
2: 5-1.6
3: 5-1.4
4: 10-2
5: 10-1.6
6: 10-1.4
7: 15-2
8: 15-1.6
9: 15-1.4
Air sampled by the probe in
cft/min.x 10^{-4}
80
70
60
50
40
30
20
10
5
4
8
9
7
1
6
2
3
.734
.534
.333
.1178
0
.066
.266
.467
.666
.866
r/R

Fig.5.

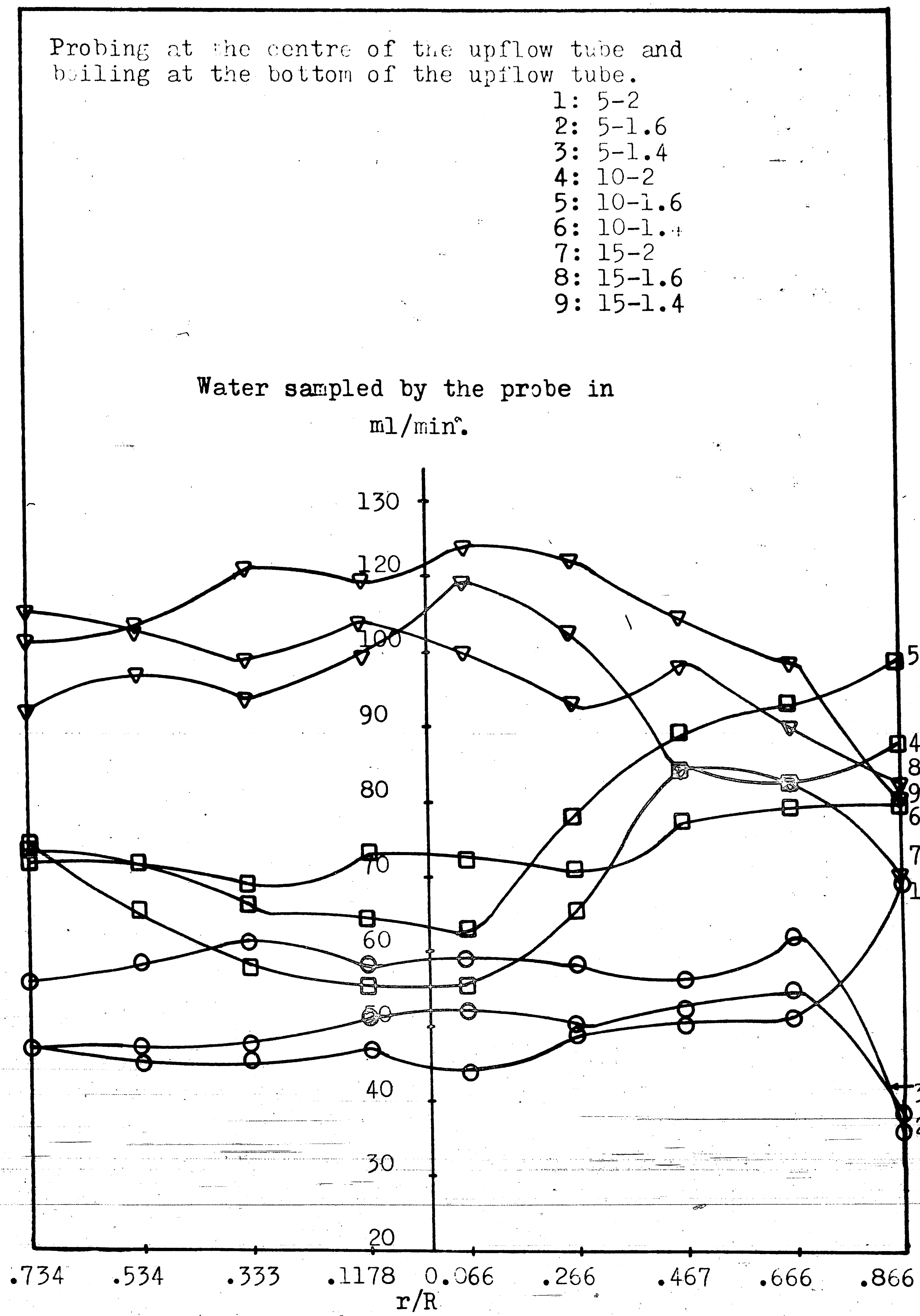
Probing at the centre of the upflow tube and boiling at the bottom of the upflow tube.
1: 5-2
2: 5-1.6
3: 5-1.4
4: 10-2
5: 10-1.6
6: 10-1.4
7: 15-2
8: 15-1.6
9: 15-1.4
Water sampled by the probe in ml/min.
130
120
100
90
80
70
60
50
40
30
20
5
4
8
9
6
7
1
3
2
.734
.534
.333
.1178
0.066
.266
.467
.666
.866
r/R

Fig.6.

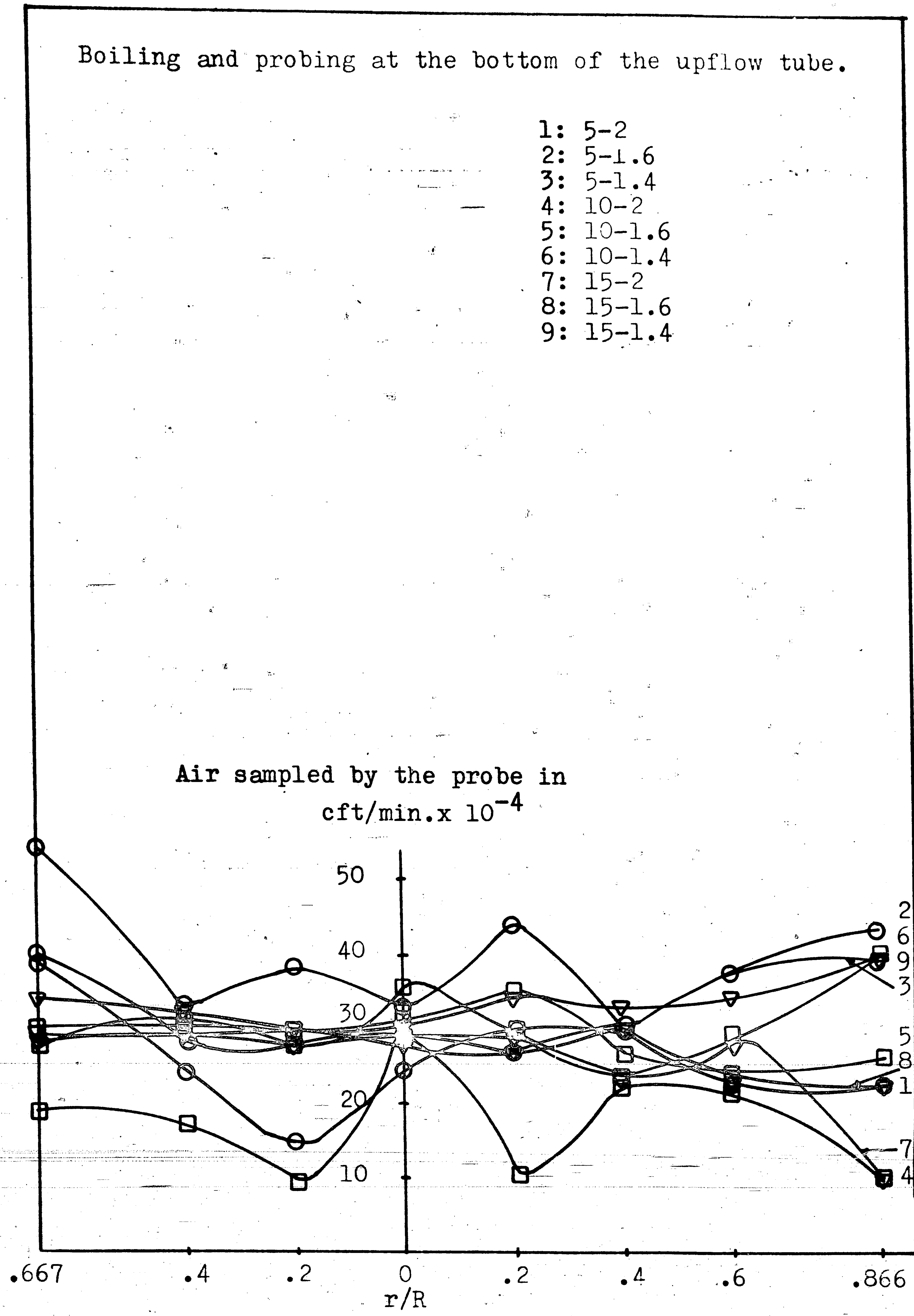
Boiling and probing at the bottom of the upflow tube.
1: 5-2
2: 5-1.6
3: 5-1.4
4: 10-2
5: 10-1.6
6: 10-1.4
7: 15-2
8: 15-1.6
9: 15-1.4
Air sampled by the probe in
cft/min.x 10-4
50
40
30
20
10
2
6
9
3
5
8
1
7
4
.667
.4
.2
0
.2
.4
.6
.866
r/R

Fig.7.

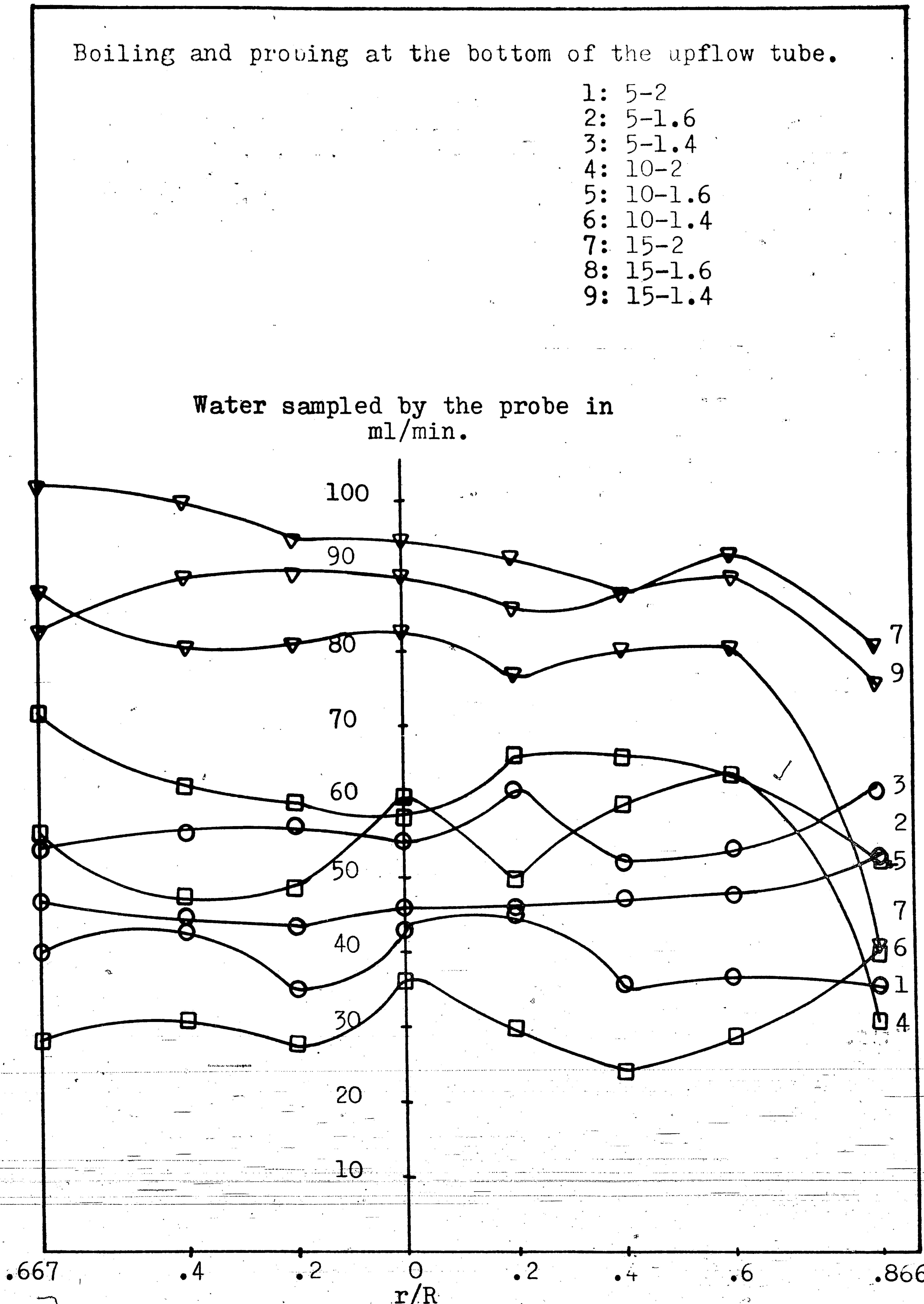

Boiling and probing at the bottom of the upflow tube.
1: 5-2
2: 5-1.6
3: 5-1.4
4: 10-2
5: 10-1.6
6: 10-1.4
7: 15-2
8: 15-1.6
9: 15-1.4
Water sampled by the probe in ml/min.
100
90
80
70
60
50
40
30
20
10
7
9
3
2
5
7
6
1
4
.667
.4
.2
0
.2
.4
.6
.866
r/R

Fig.8.

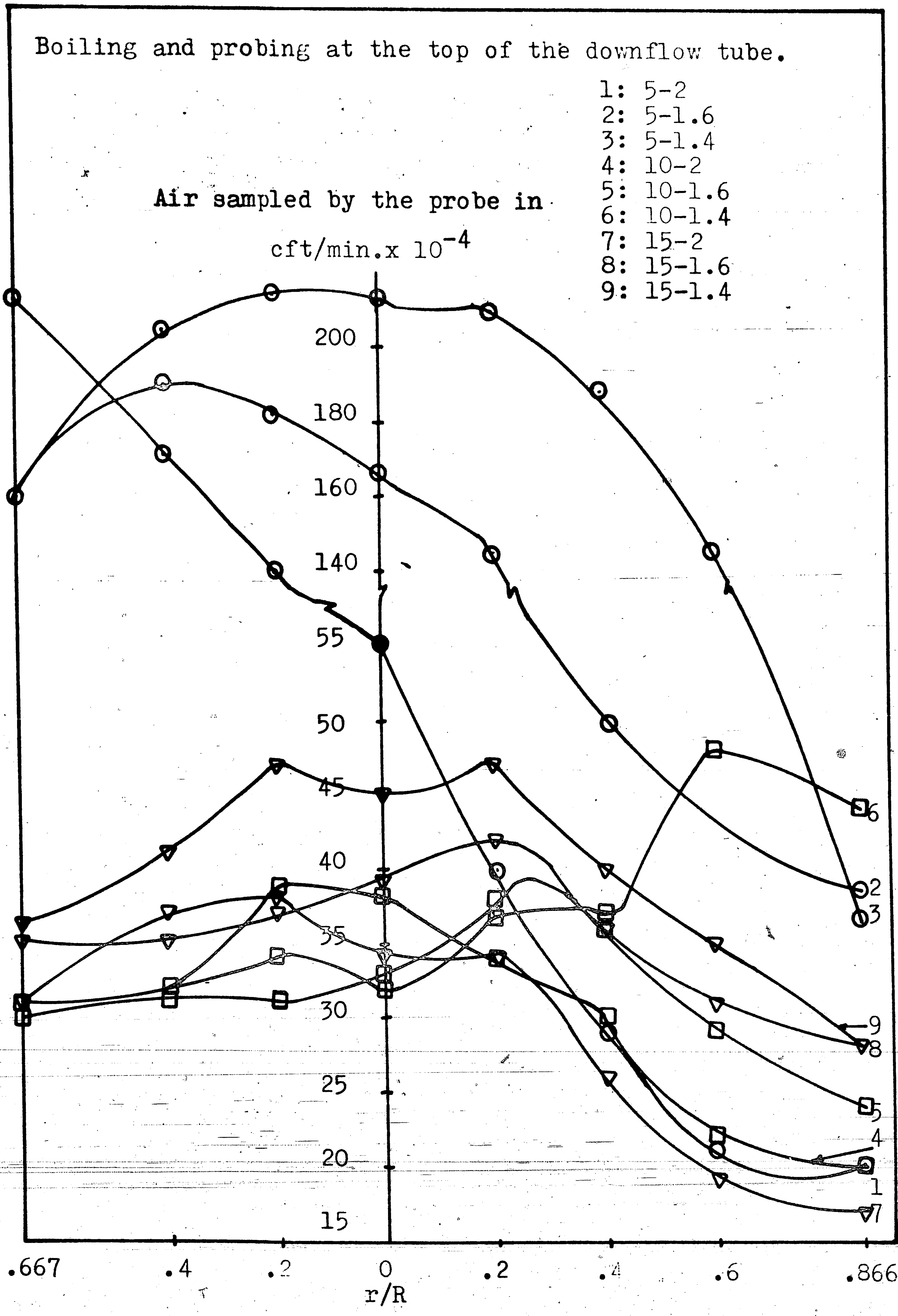
Boiling and probing at the top of the downflow tube.
1: 5-2
2: 5-1.6
3: 5-1.4
4: 10-2
5: 10-1.6
6: 10-1.4
7: 15-2
8: 15-1.6
9: 15-1.4
Air sampled by the probe in
cft/min.x 10^{-4}
200
180
160
140
55
50
45
40
35
30
25
20
15
.667
.4
.2
0
.2
.4
.6
.866
r/R

Fig.9.

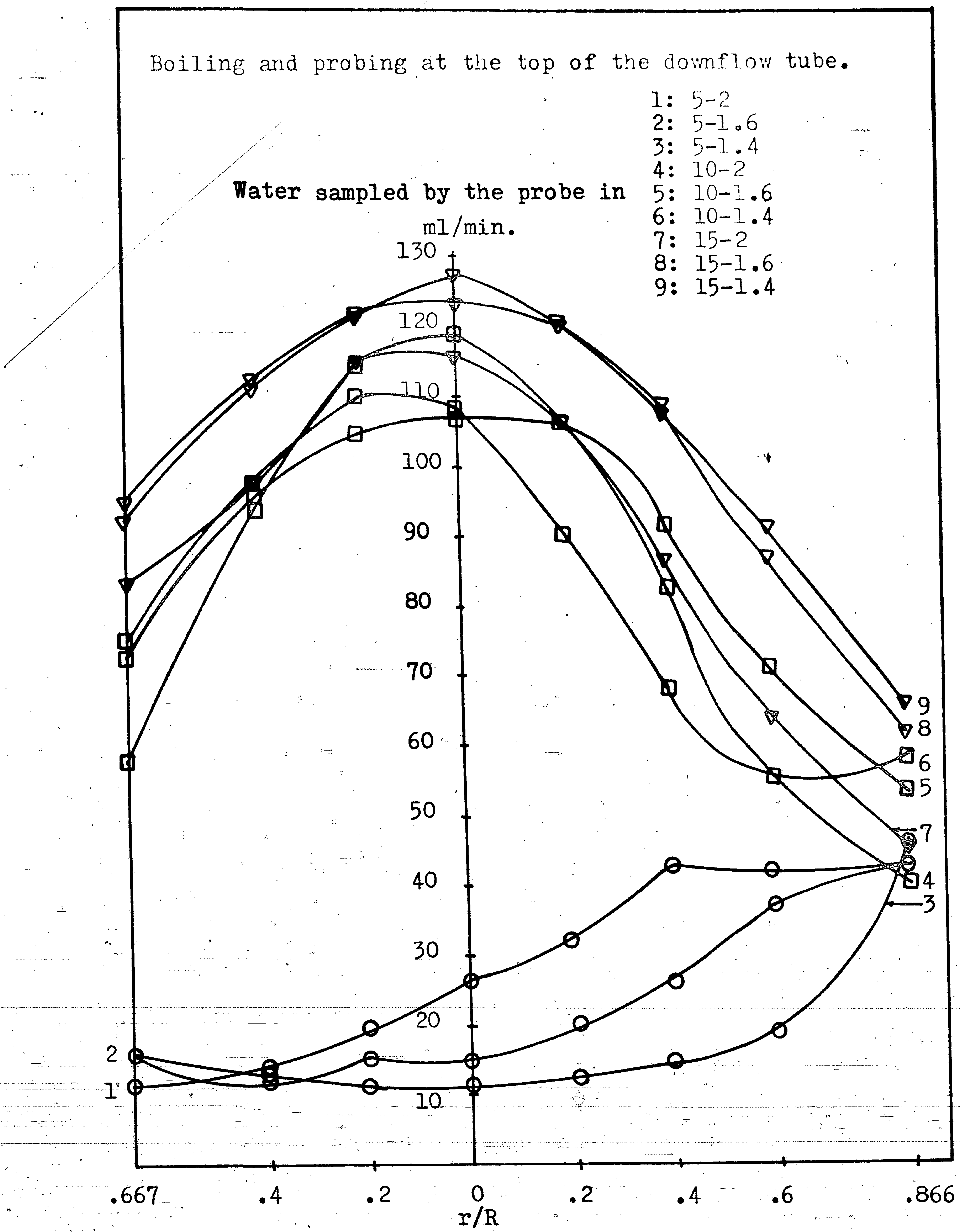
Boiling and probing at the top of the downflow tube.
1: 5-2
2: 5-1.6
3: 5-1.4
4: 10-2
5: 10-1.6
6: 10-1.4
7: 15-2
8: 15-1.6
9: 15-1.4
Water sampled by the probe in ml/min.
130
120
110
100
90
80
70
60
50
40
30
20
10
.667
.4
.2
0
.2
.4
.6
.866
r/R

Fig.10.

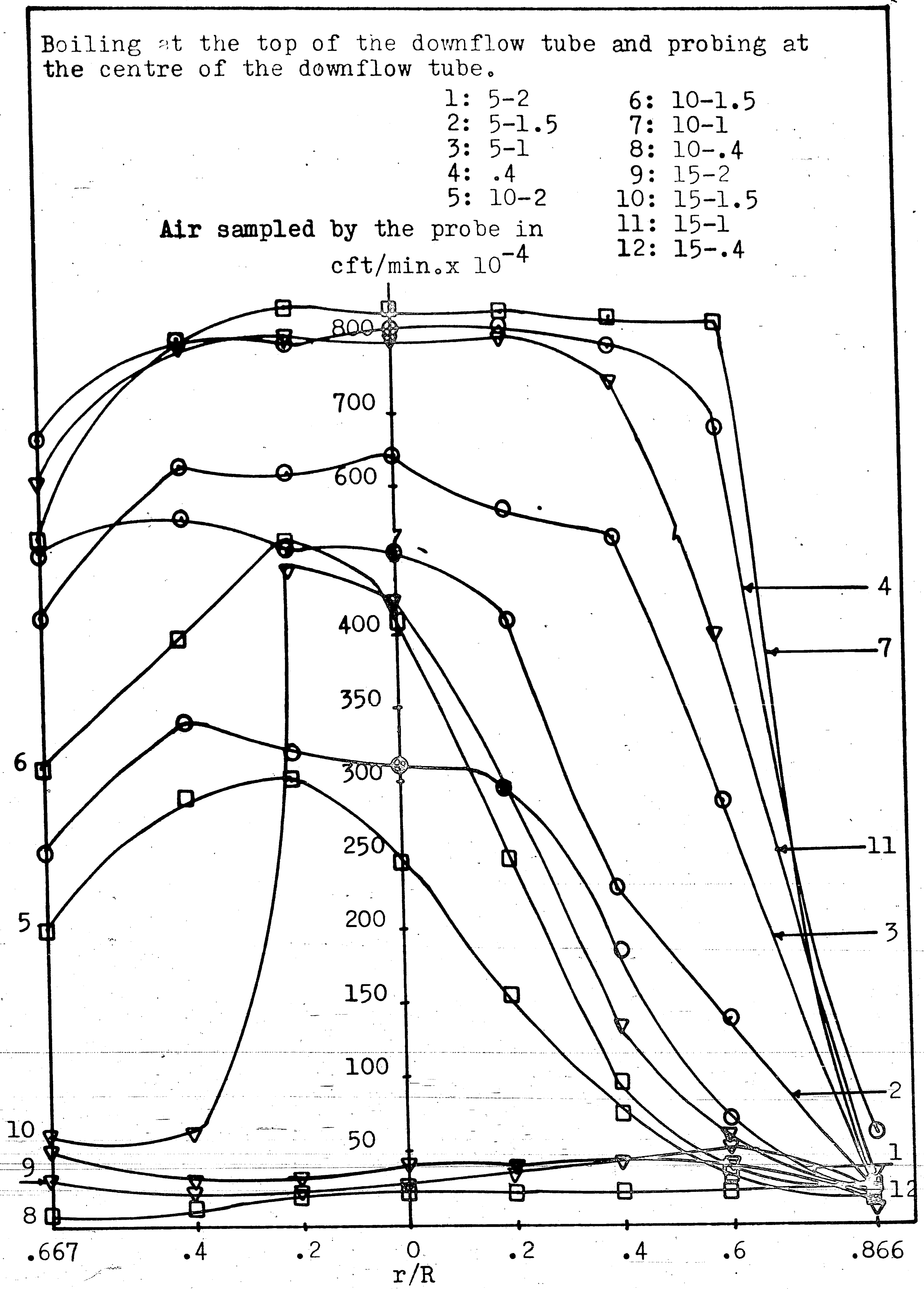
Boiling at the top of the downflow tube and probing at the centre of the downflow tube.
1: 5-2
2: 5-1.5
3: 5-1
4: .4
5: 10-2
6: 10-1.5
7: 10-1
8: 10-.4
9: 15-2
10: 15-1.5
11: 15-1
12: 15-.4
Air sampled by the probe in cft/min.x 10^-4
800
700
600
400
350
300
250
200
150
100
50
.667
.4
.2
0
.2
.4
.6
.866
r/R

Fig.11.

Boiling at the top of the downflow tube and probing at the centre of the downflow tube.

1: 5-2
2: 5-1.5
3: 5-1
4: 5-.4
5: 10-2
6: 10-1.5
7: 10-1
8: 10-.4
9: 15-2
10: 15-1.5
11: 15-1

Water sampled by the probe in ml/min.

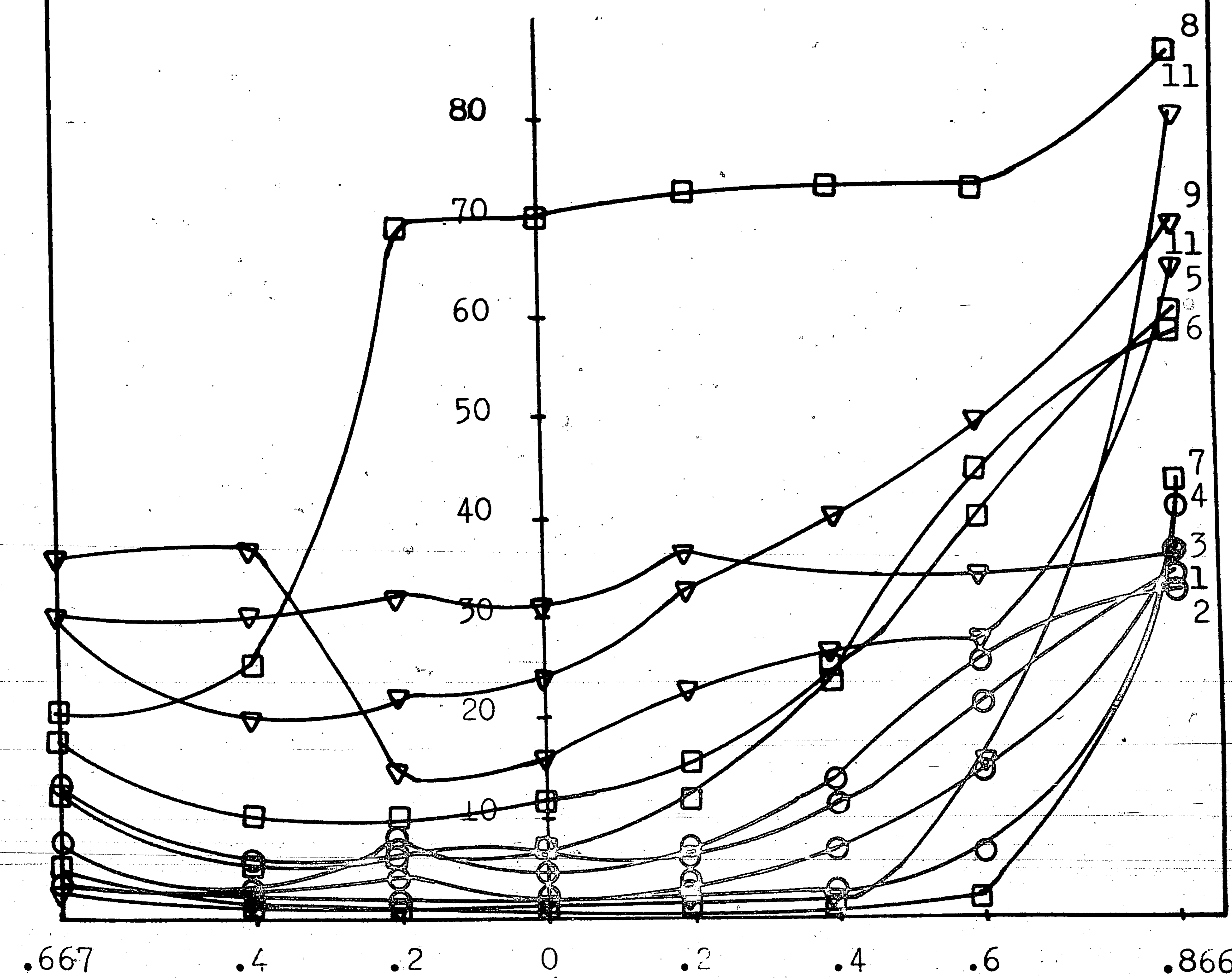

r/R

Fig.12.

Boiling at the top of the downflowtube and probing at the centre of the downflow tube.

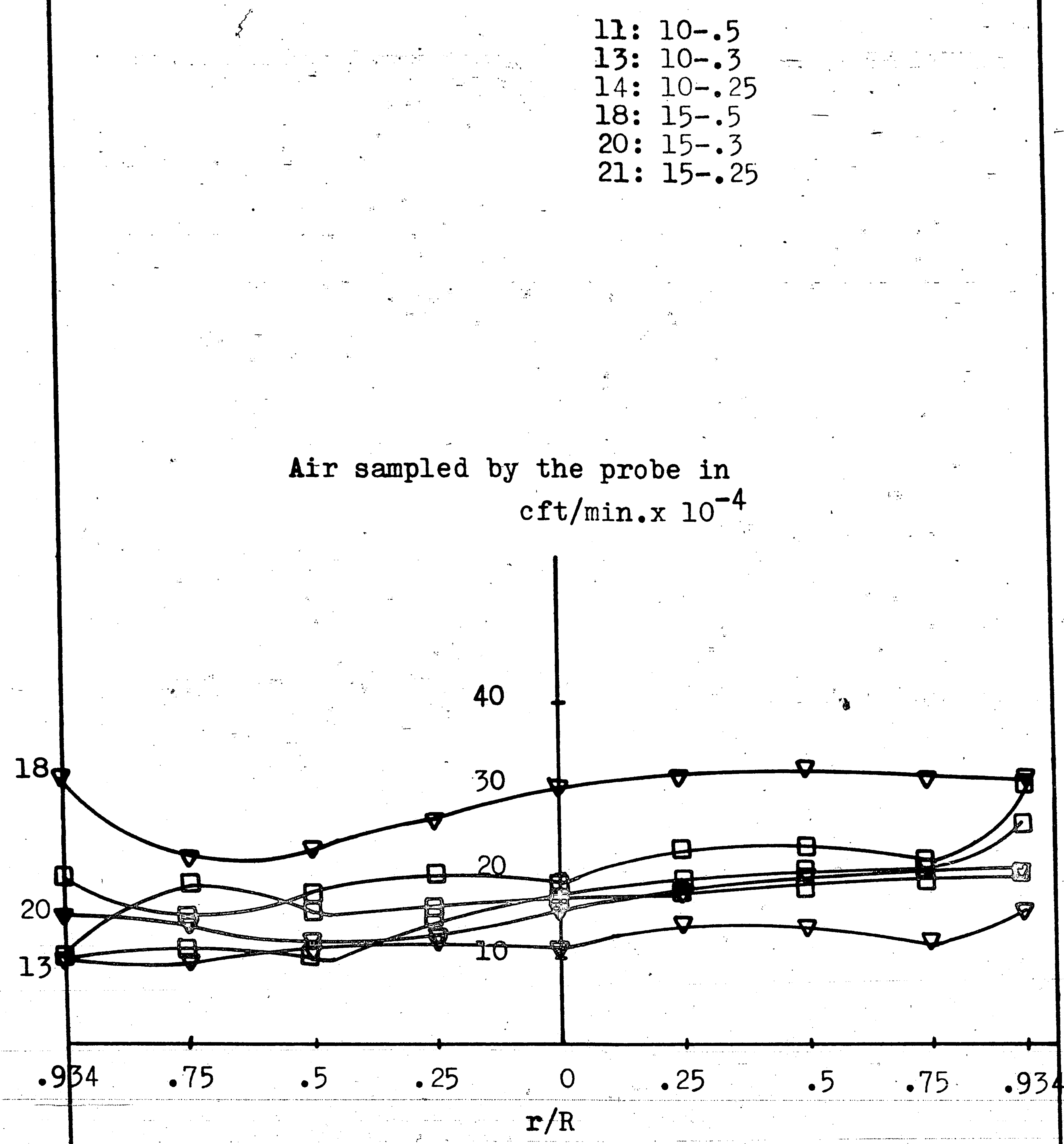

Fig.13(a).

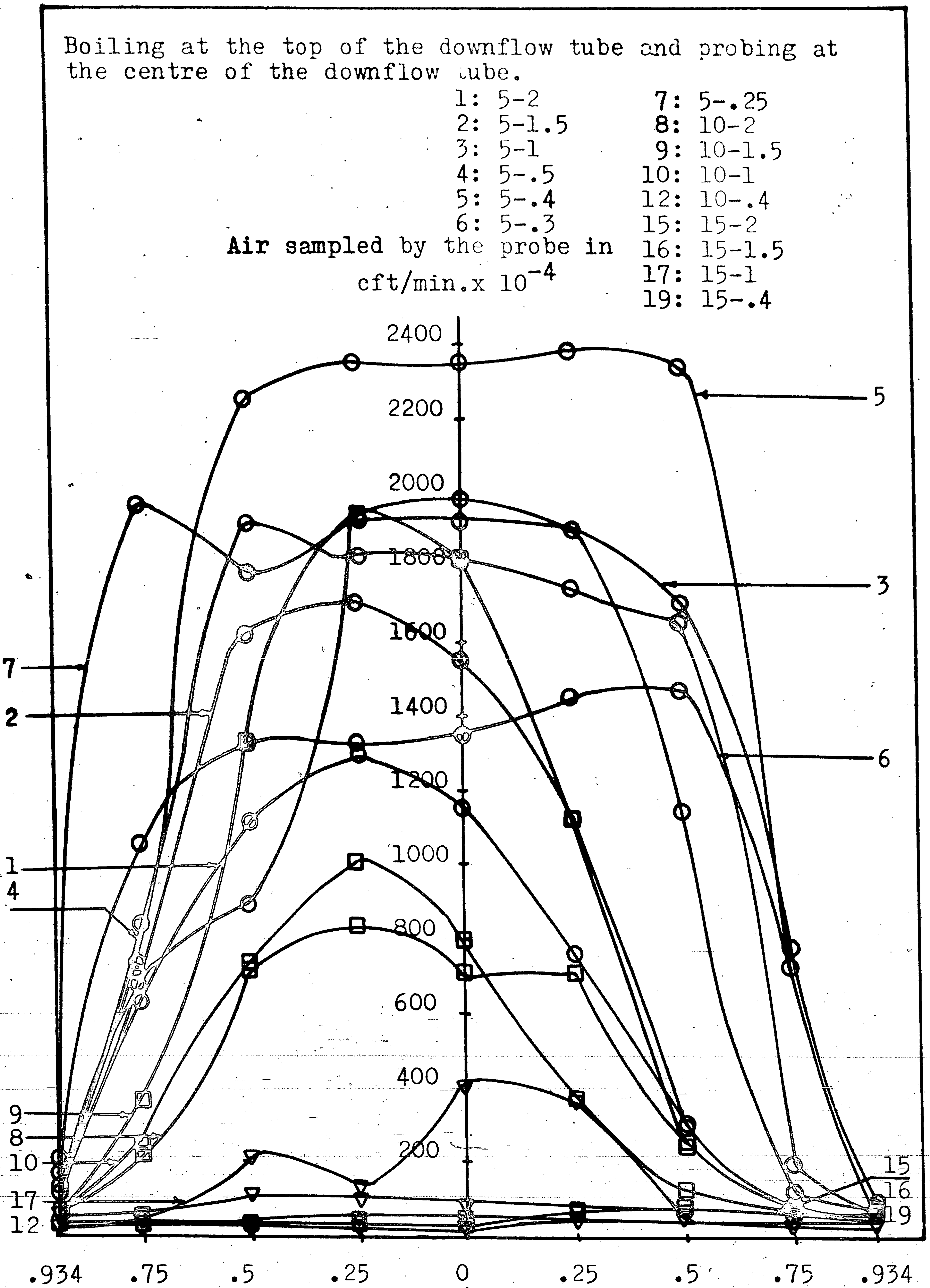

Boiling at the top of the downflow tube and probing at the centre of the downflow tube.
1: 5-2
2: 5-1.5
3: 5-1
4: 5-.5
5: 5-.4
6: 5-.3
7: 5-.25
8: 10-2
9: 10-1.5
10: 10-1
12: 10-.4
15: 15-2
16: 15-1.5
17: 15-1
19: 15-.4
Air sampled by the probe in cft/min.x 10^{-4}
2400
2200
2000
1800
1600
1400
1200
1000
800
600
400
200
.934
.75
.5
.25
0
.25
.5
.75
.934
r/R

Fig.13(b).

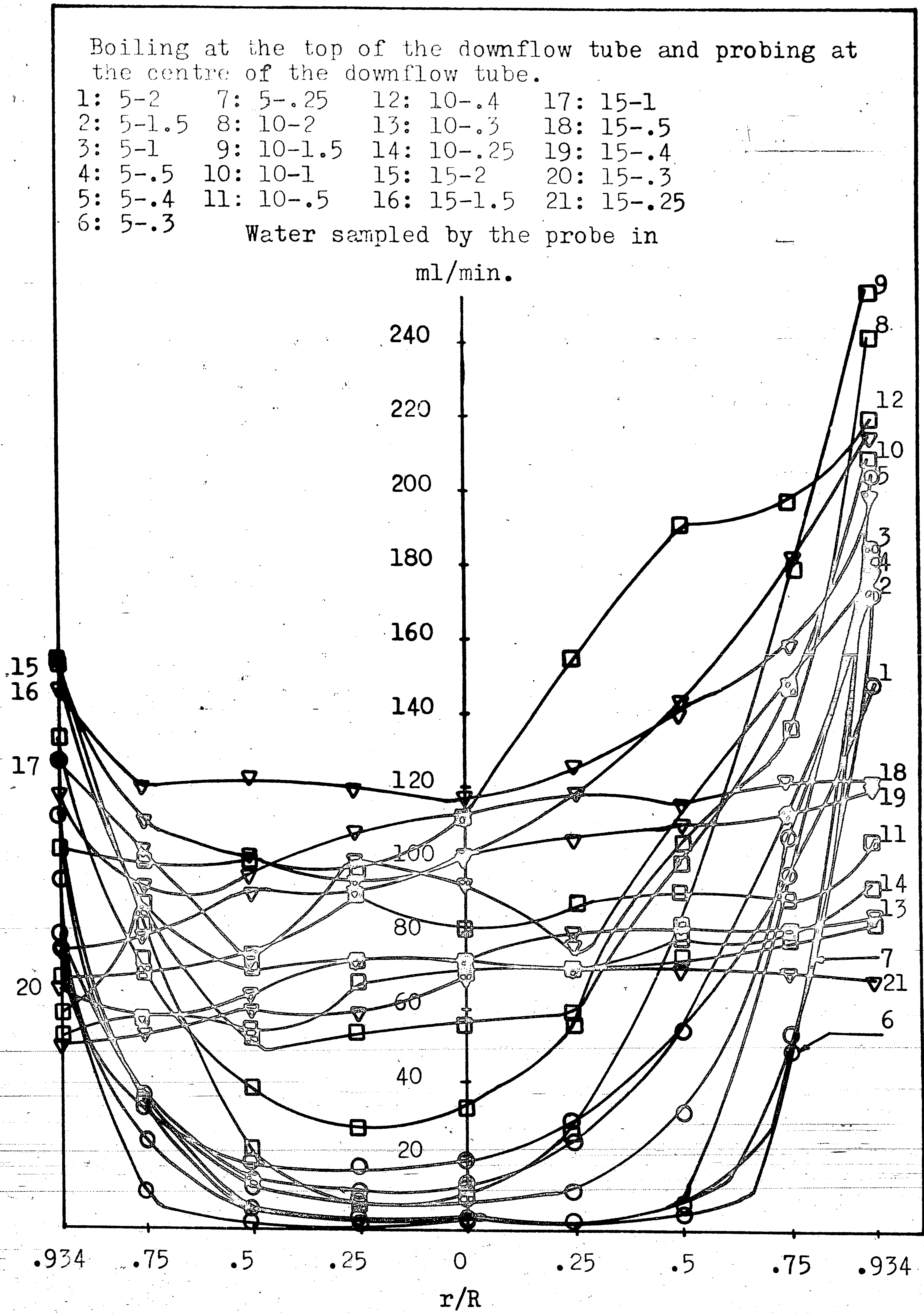
Boiling at the top of the downflow tube and probing at the centre of the downflow tube.
1: 5-2
2: 5-1.5
3: 5-1
4: 5-.5
5: 5-.4
6: 5-.3
7: 5-.25
8: 10-2
9: 10-1.5
10: 10-1
11: 10-.5
12: 10-.4
13: 10-.3
14: 10-.25
15: 15-2
16: 15-1.5
17: 15-1
18: 15-.5
19: 15-.4
20: 15-.3
21: 15-.25
Water sampled by the probe in
ml/min.
240
220
200
180
160
140
120
100
80
60
40
20
.934
.75
.5
.25
0
.25
.5
.75
.934
r/R

Fig.14.

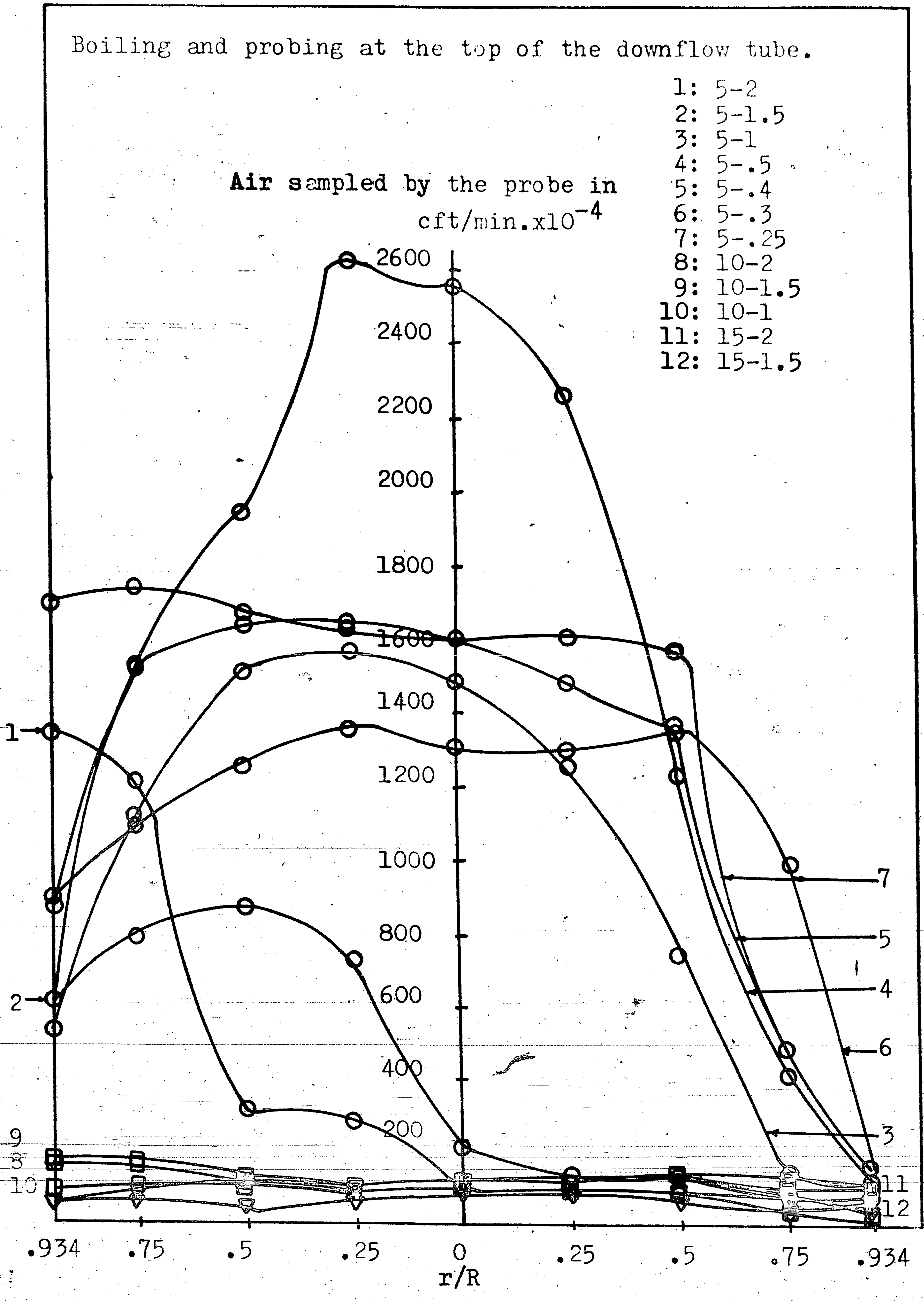
Boiling and probing at the top of the downflow tube.
1: 5-2
2: 5-1.5
3: 5-1
4: 5-.5
5: 5-.4
6: 5-.3
7: 5-.25
8: 10-2
9: 10-1.5
10: 10-1
11: 15-2
12: 15-1.5
Air sampled by the probe in cft/min.x10^{-4}
2600
2400
2200
2000
1800
1600
1400
1200
1000
800
600
400
200
.934
.75
.5
.25
0
.25
.5
.75
.934
r/R

Fig.15.

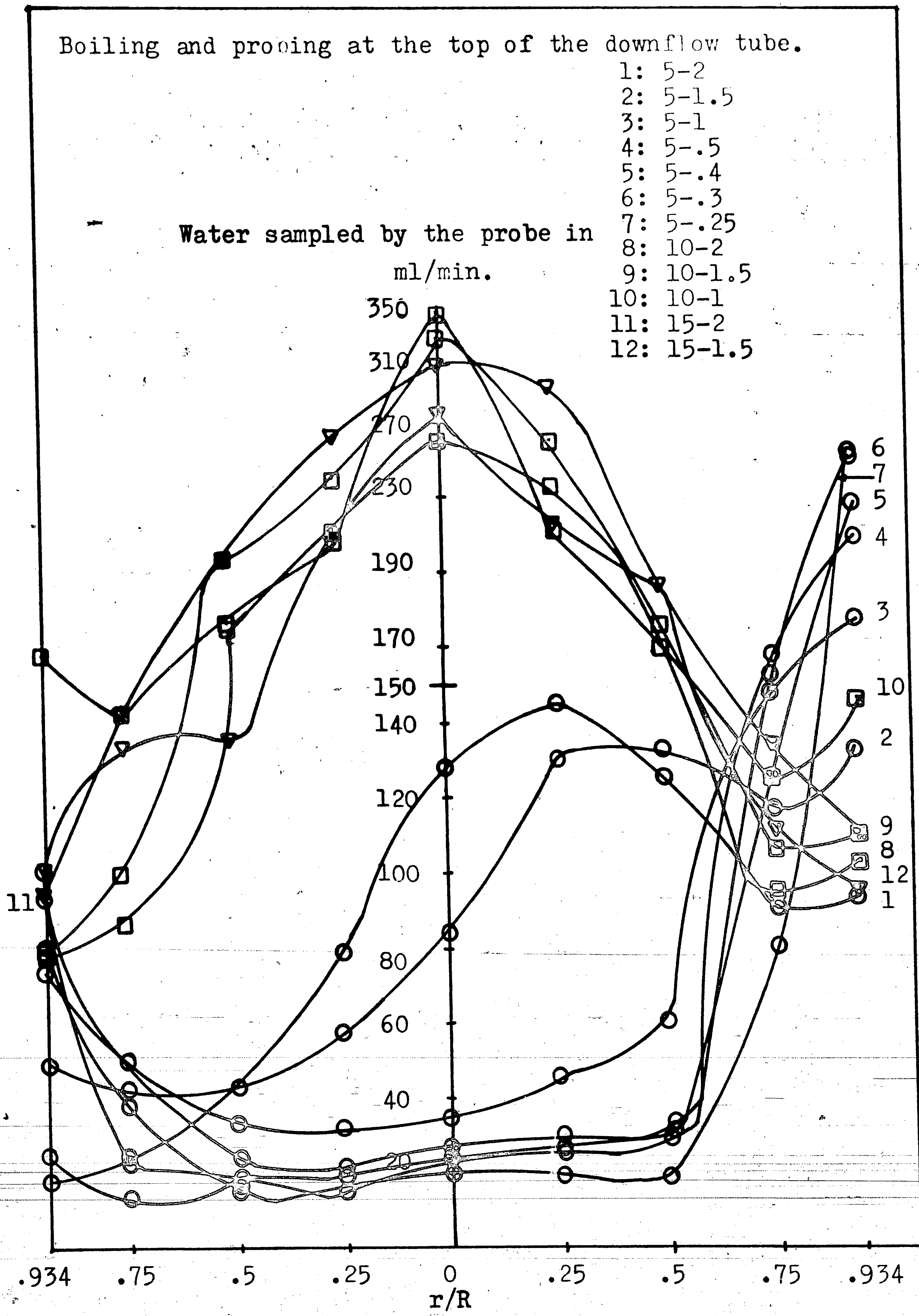
Boiling and prooing at the top of the downflow tube.
1: 5-2
2: 5-1.5
3: 5-1
4: 5-.5
5: 5-.4
6: 5-.3
7: 5-.25
8: 10-2
9: 10-1.5
10: 10-1
11: 15-2
12: 15-1.5
Water sampled by the probe in ml/min.
350
310
270
230
190
170
150
140
120
100
80
60
40
20
.934
.75
.5
.25
0
.25
.5
.75
.934
r/R

Fig.16.

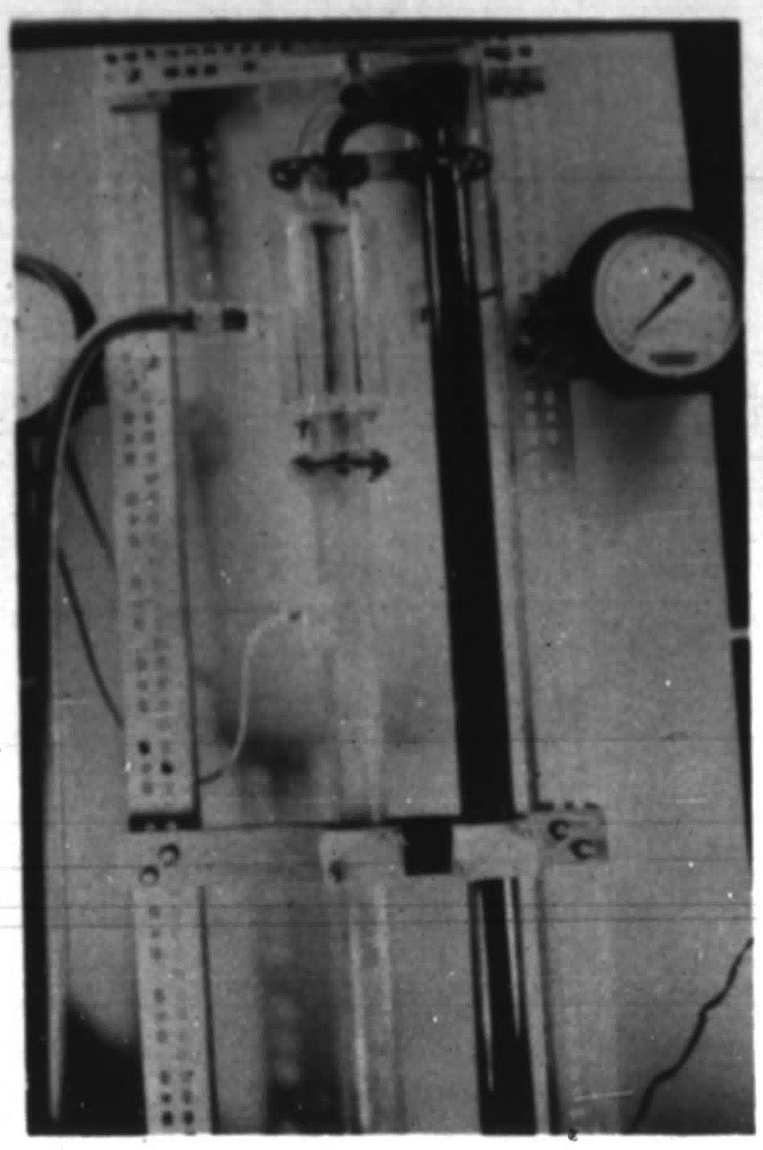

F.V.P.-A.B.2-W.3

Fig. 17.

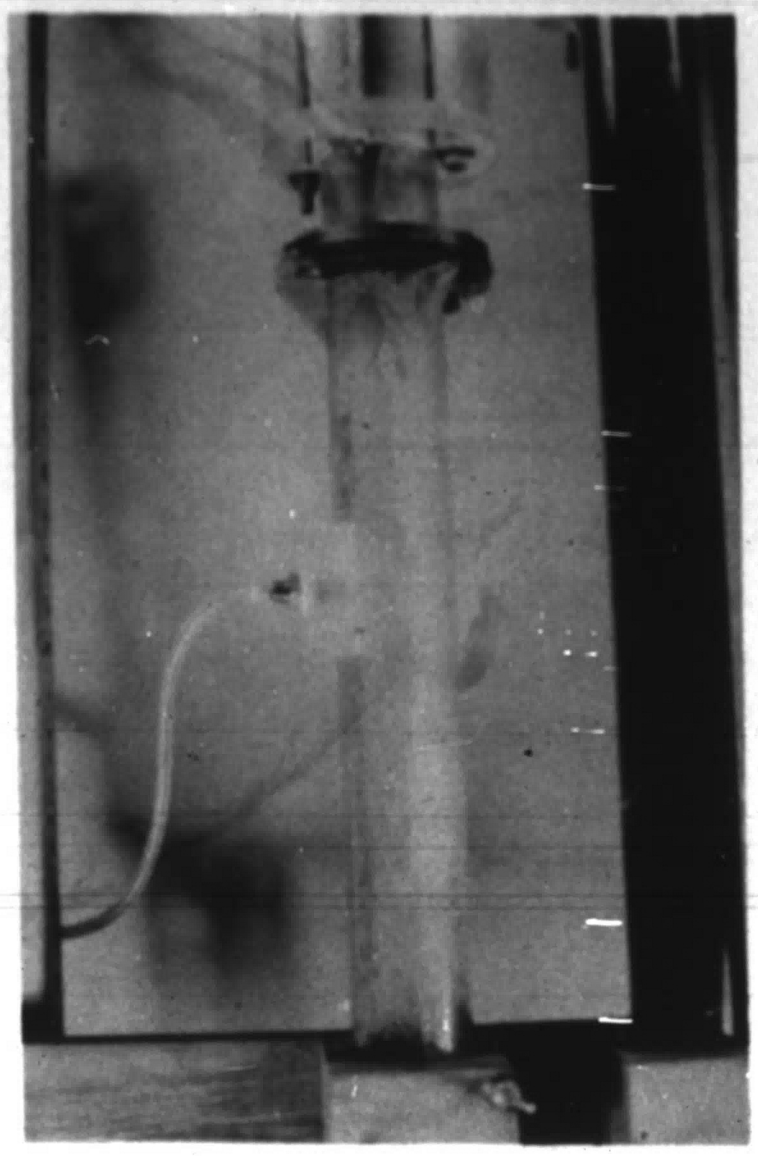

C.V.P.-A.B.2-W.3

Fig. 18.

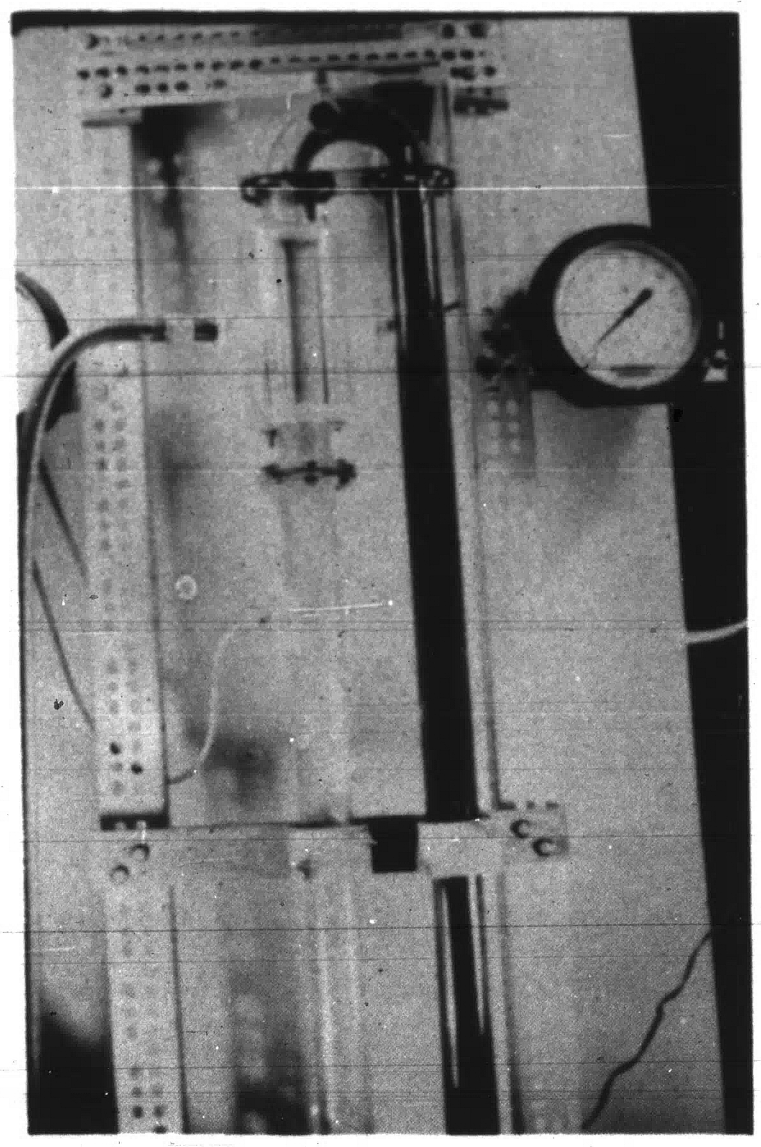

F.V.P.-A.B.2-W.4

Fig. 19.

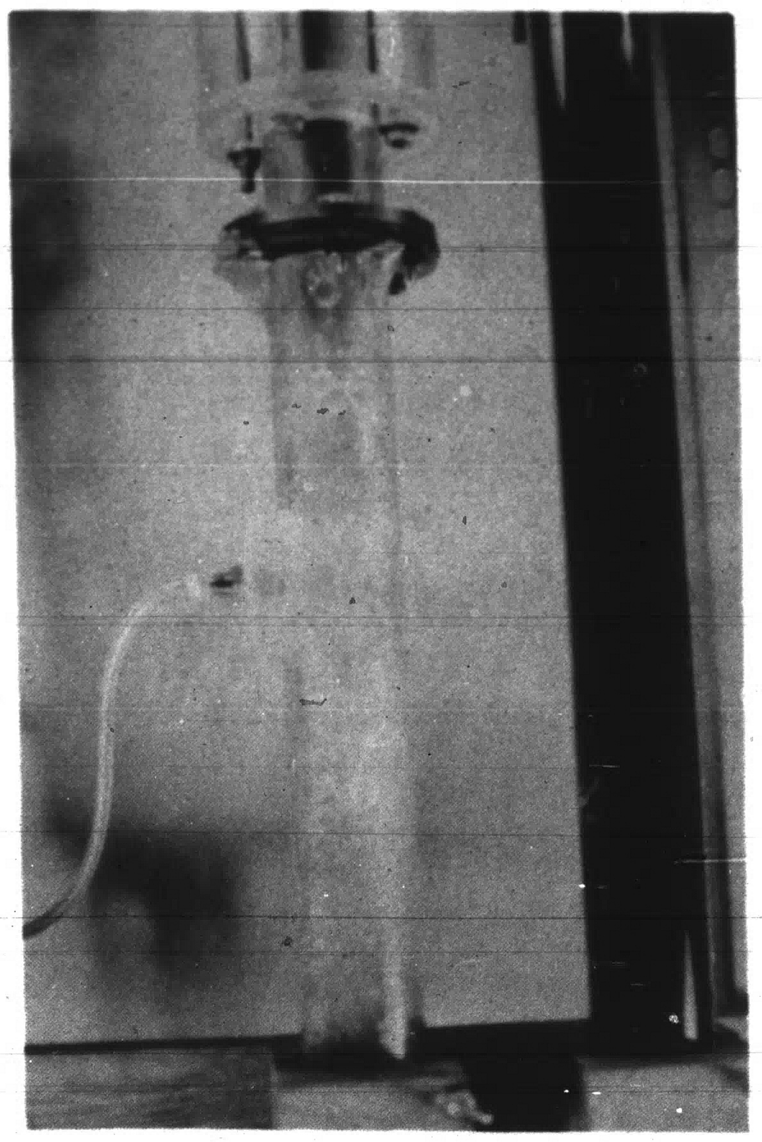

C.V.P.-A.B.2-W.4

Fig. 20.

Fig. 17-20.

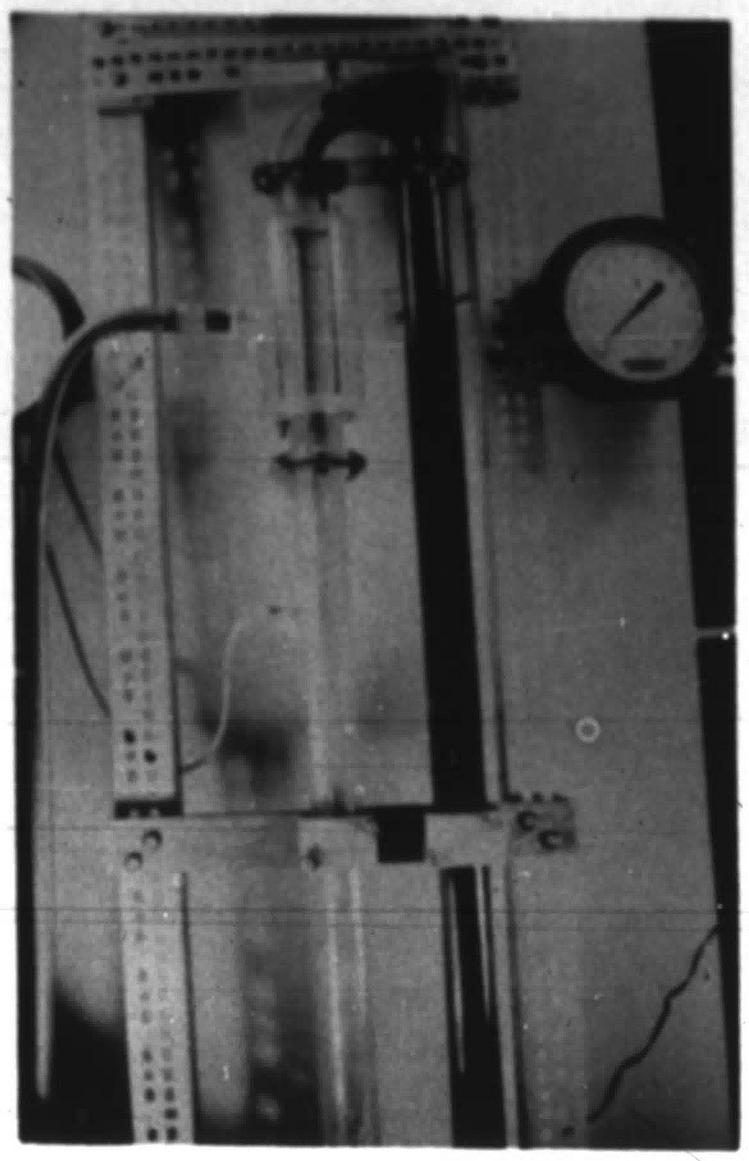

F.V.P.-A.B.2-W.5

Fig. 21.

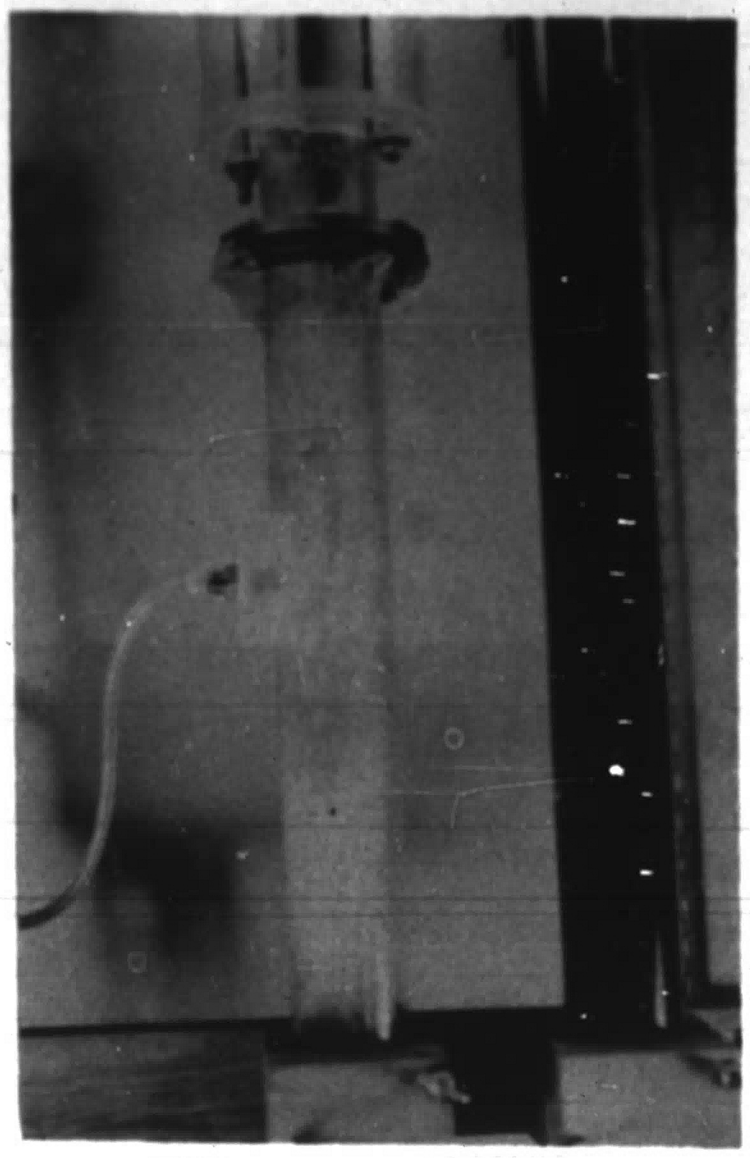

C.V.P.-A.B.2-W.5

Fig. 22.

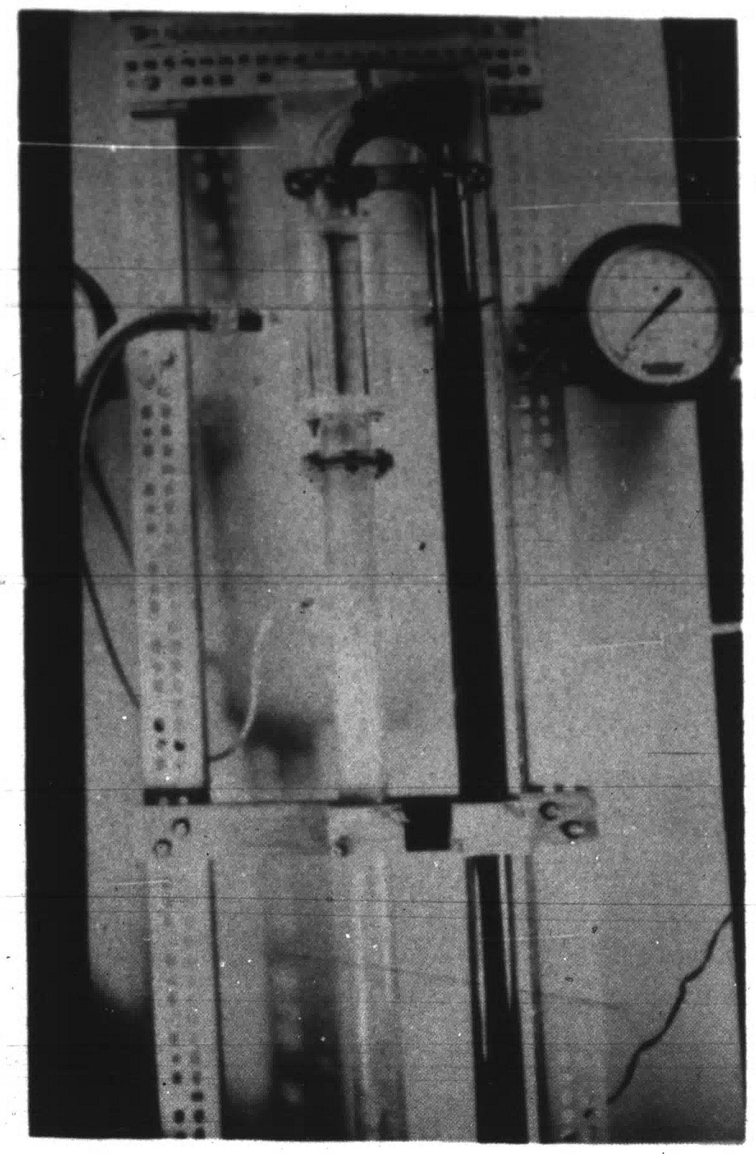

F.V.P.-A.B.2-W.6

Fig. 23.

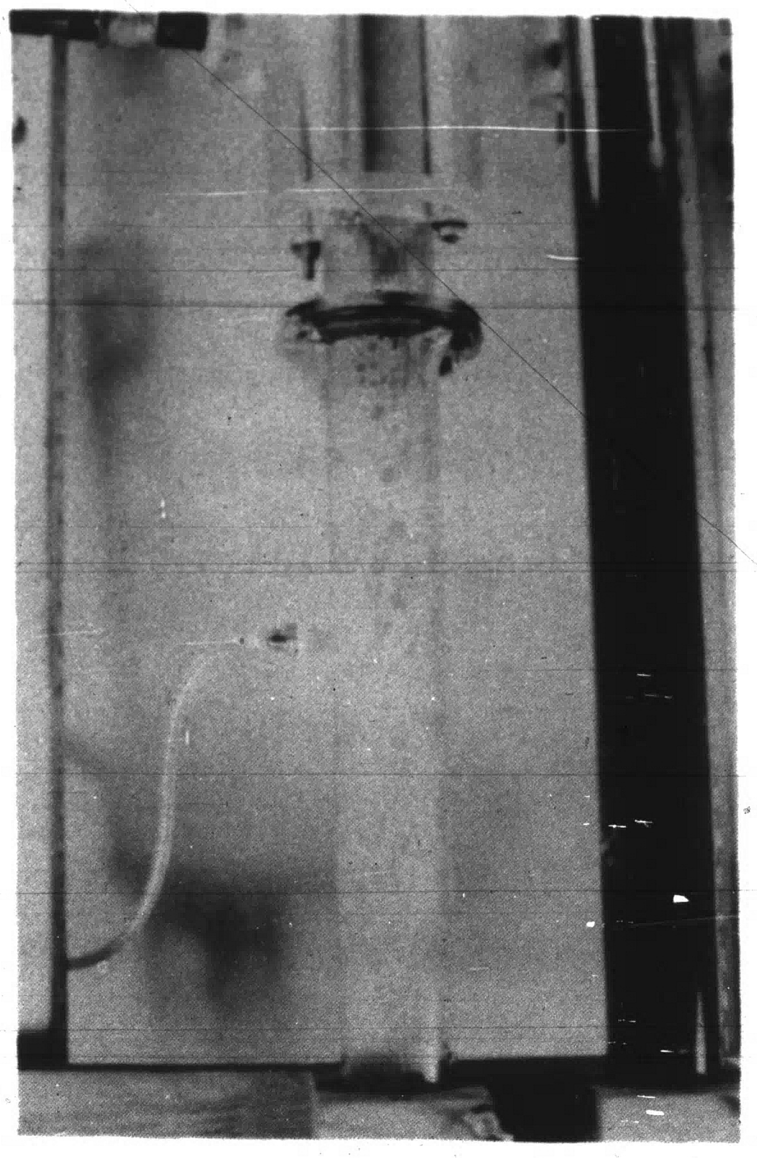

C.V.P.-A.B.2-W.6

Fig. 24.

Fig. 21-24.

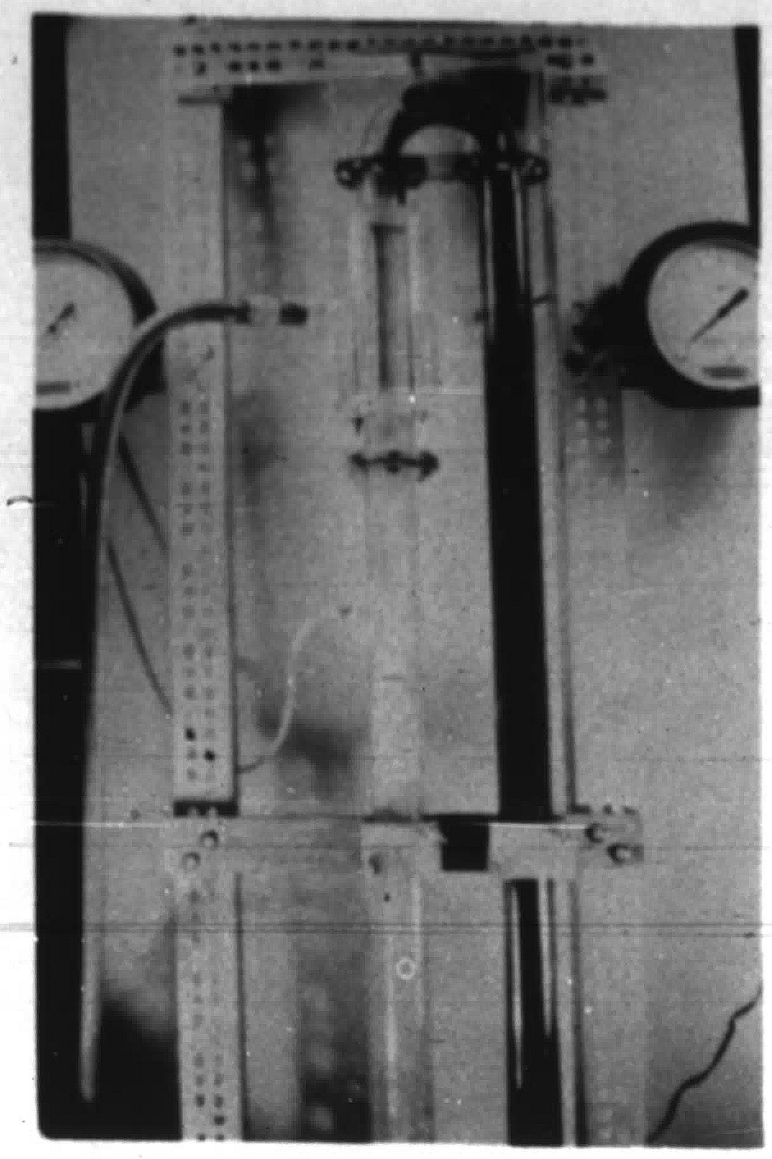

F.V.P.-A.B.2-W.6.5

Fig. 25.

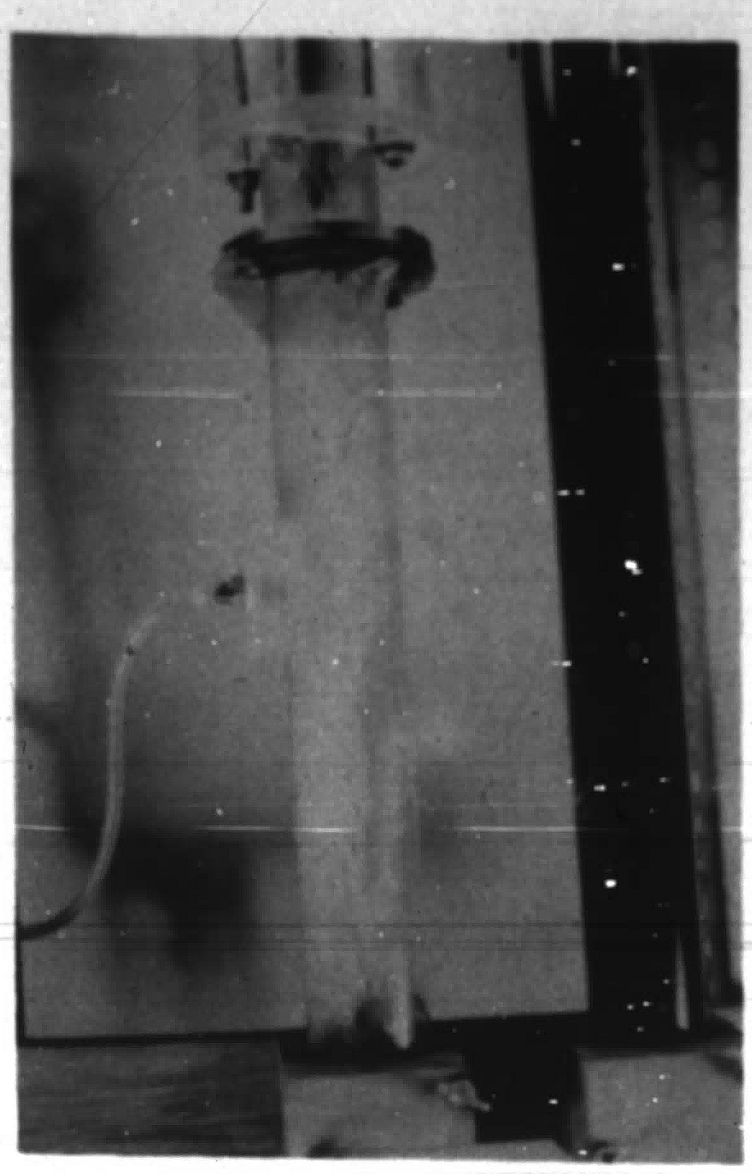

C.V.P.-A.B.2-W.6.5

Fig. 26.

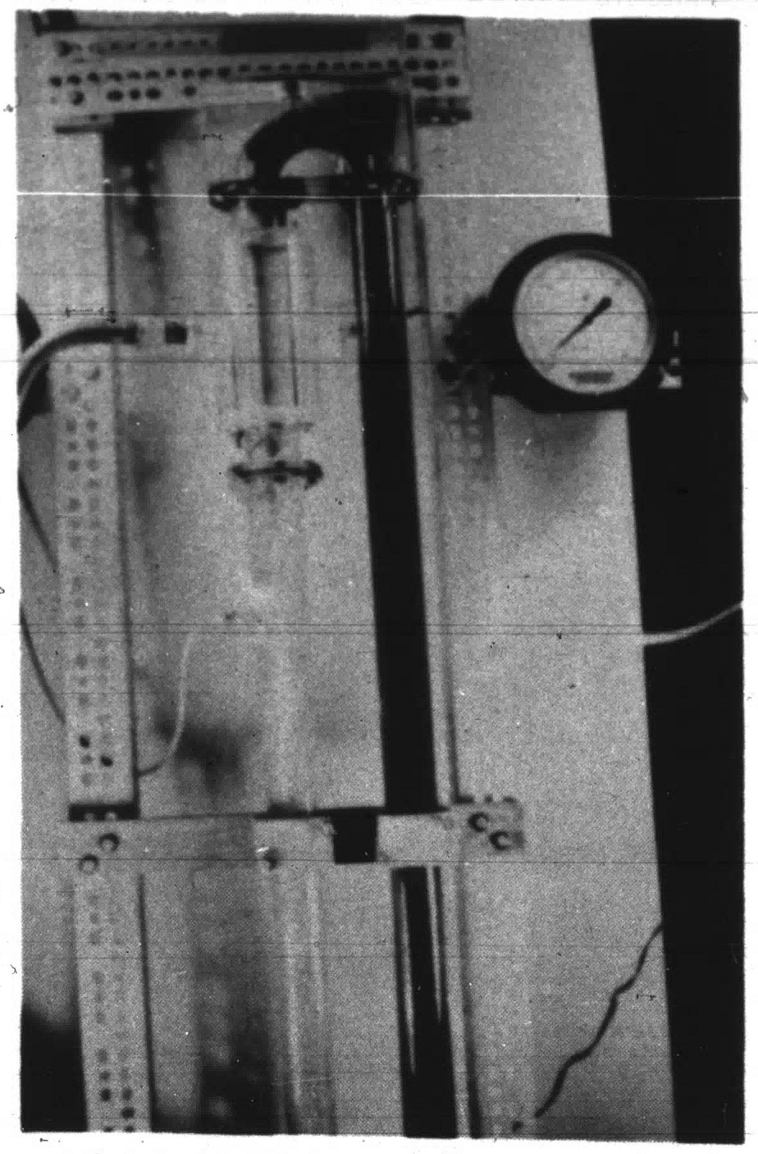

F.V.P.-A.B.2-W.7

Fig. 27.

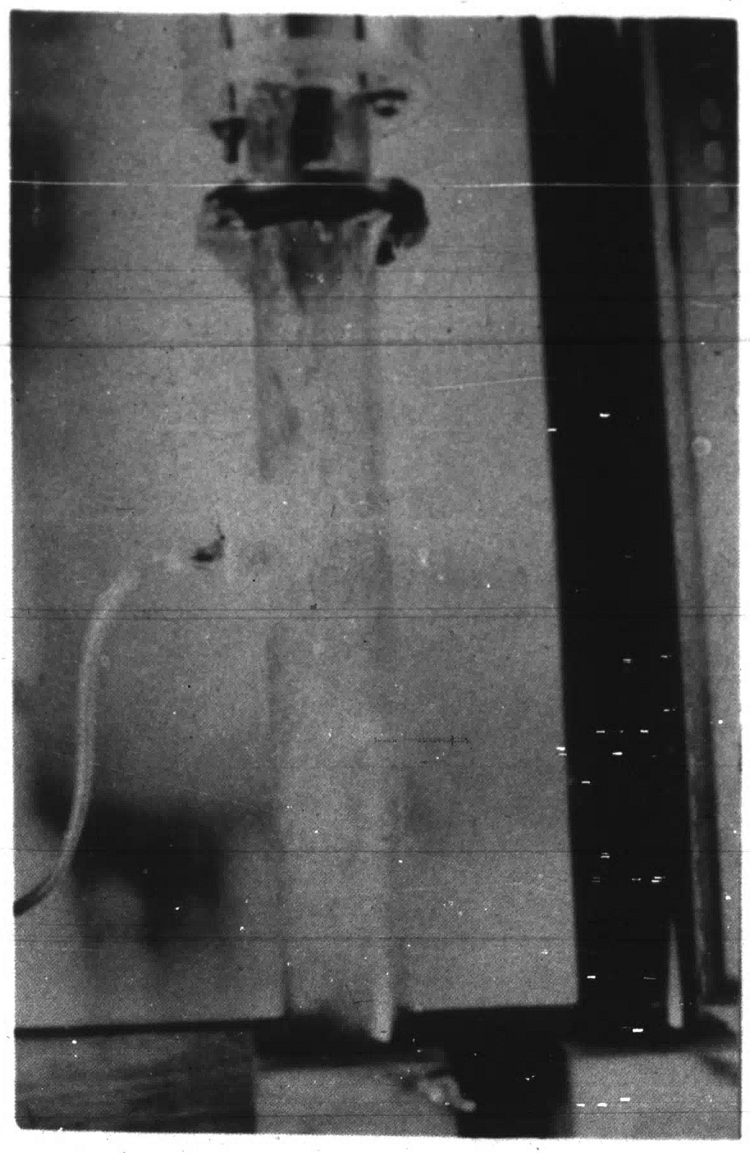

C.V.P.-A.B.2-W.7

Fig. 28.

Fig. 25-28.

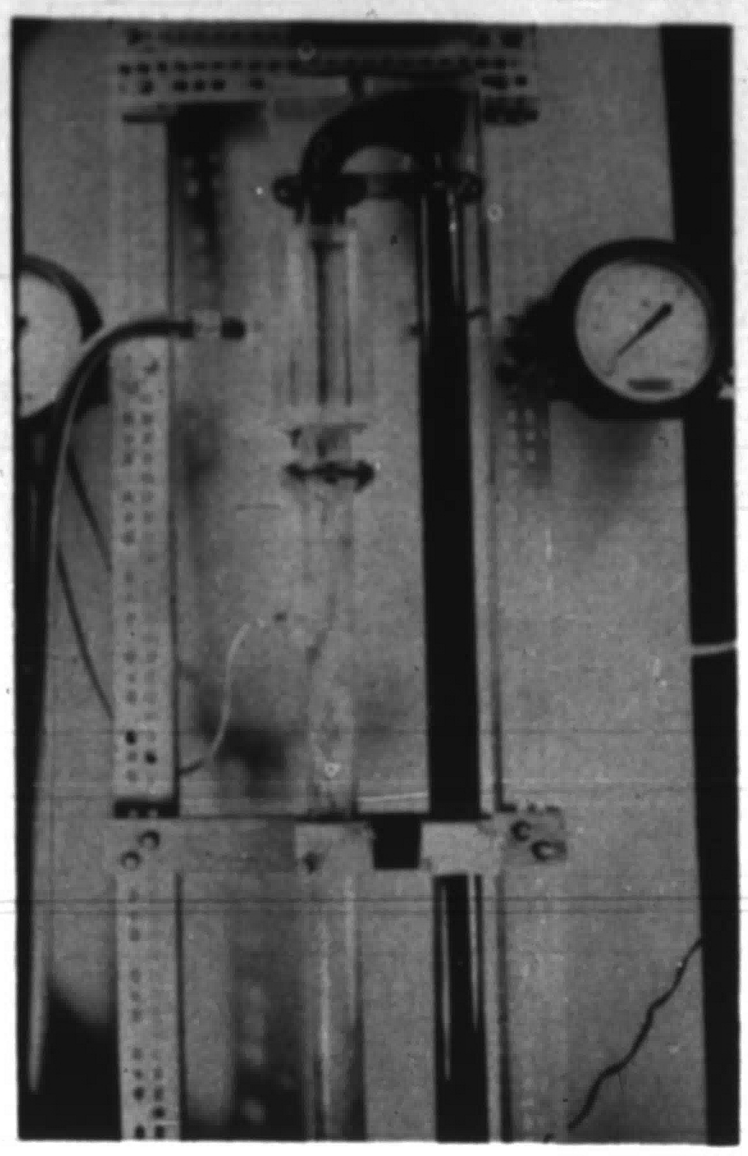

F.V.P.-A.B.2-W.7.5

Fig. 29.

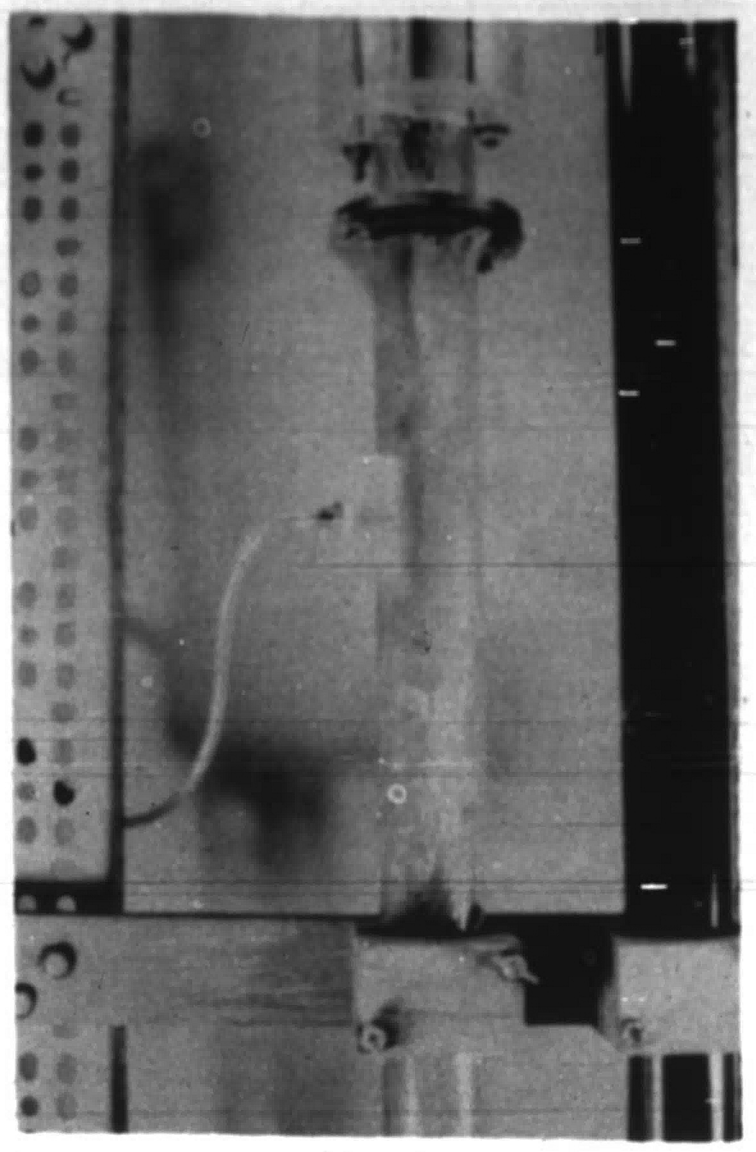

C.V.P.-A.B.2-W.7.5

Fig. 30.

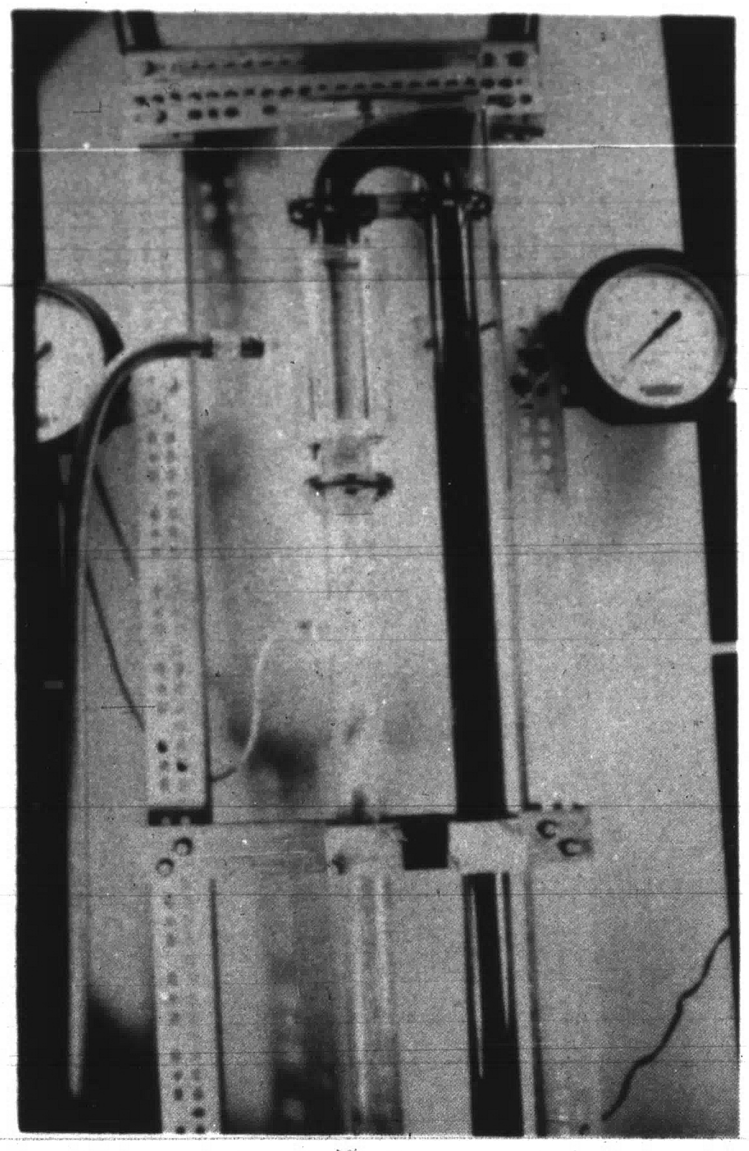

F.V.P.-A.B.2-W.8

Fig. 31.

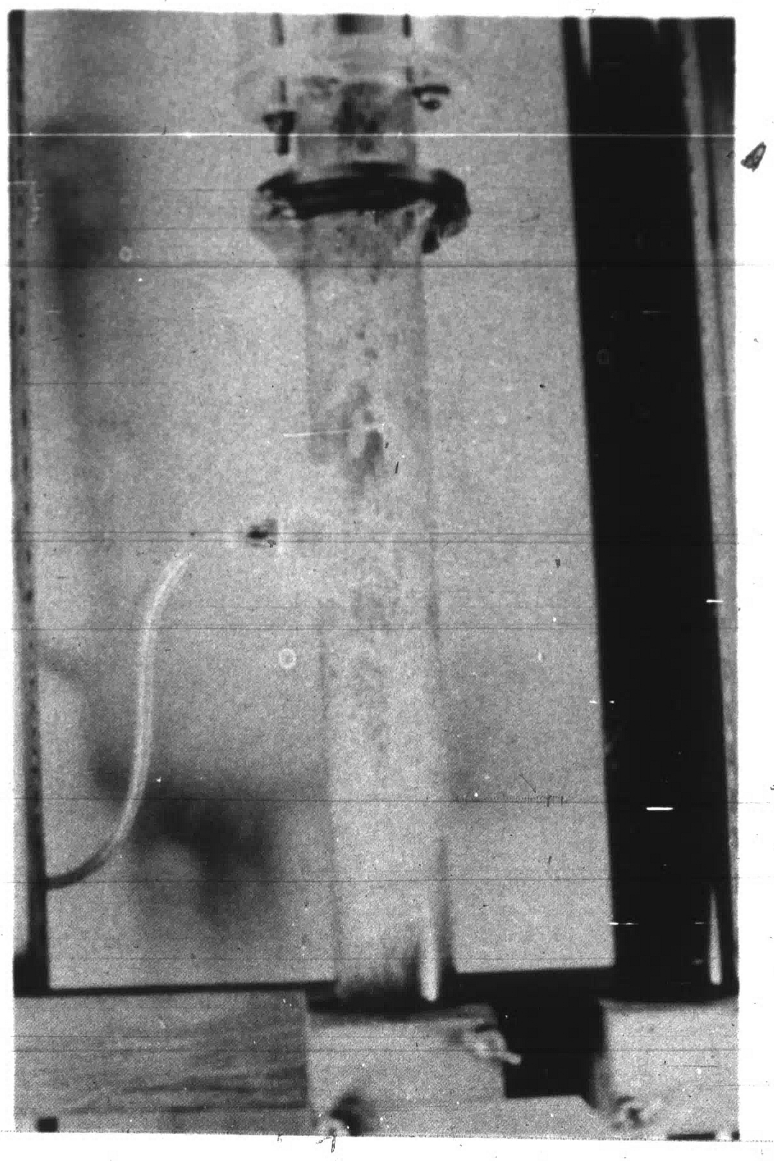

C.V.P.-A.B.2-W.8

Fig. 32.

Fig. 29-32.

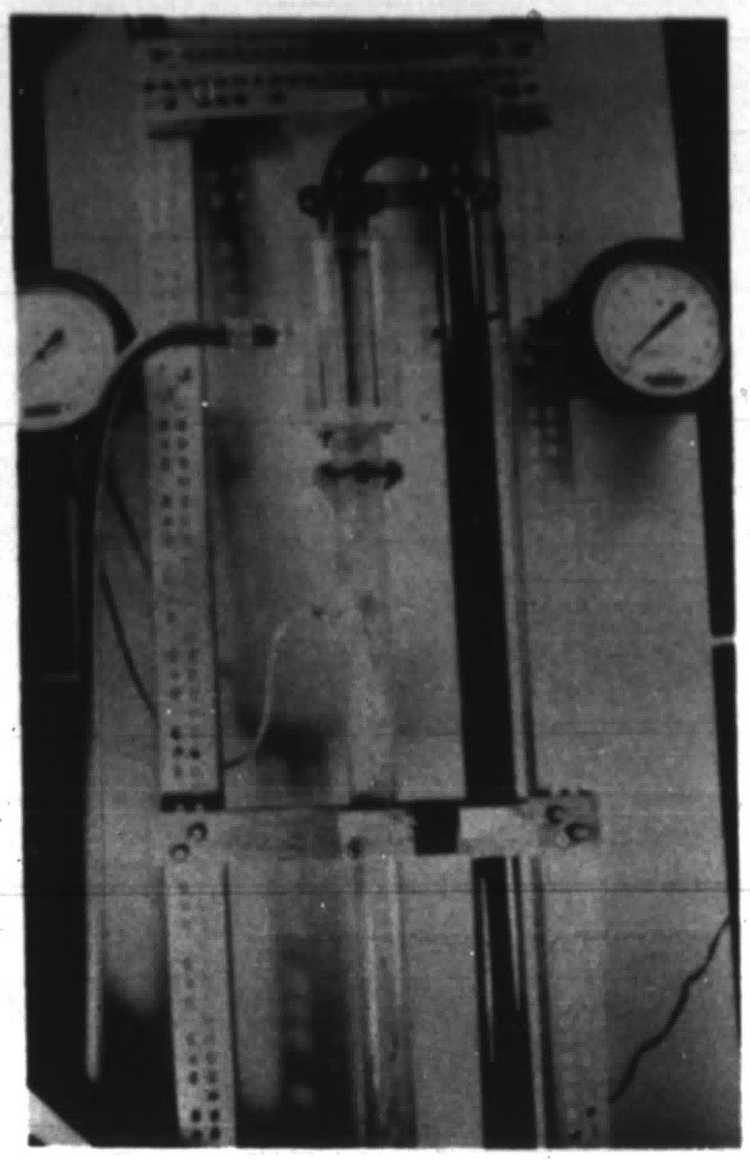

F.V.P.-A.B.2-W.10

Fig. 33.

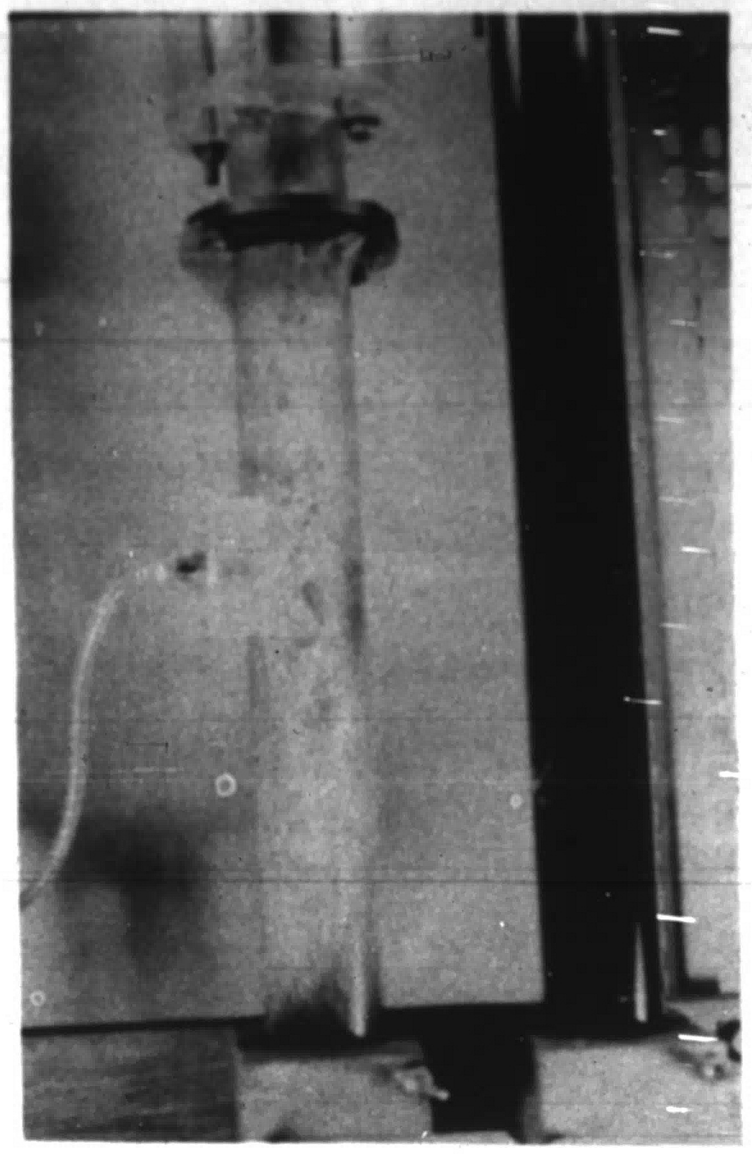

C.V.P.-A.B.2-W.10

Fig. 34.

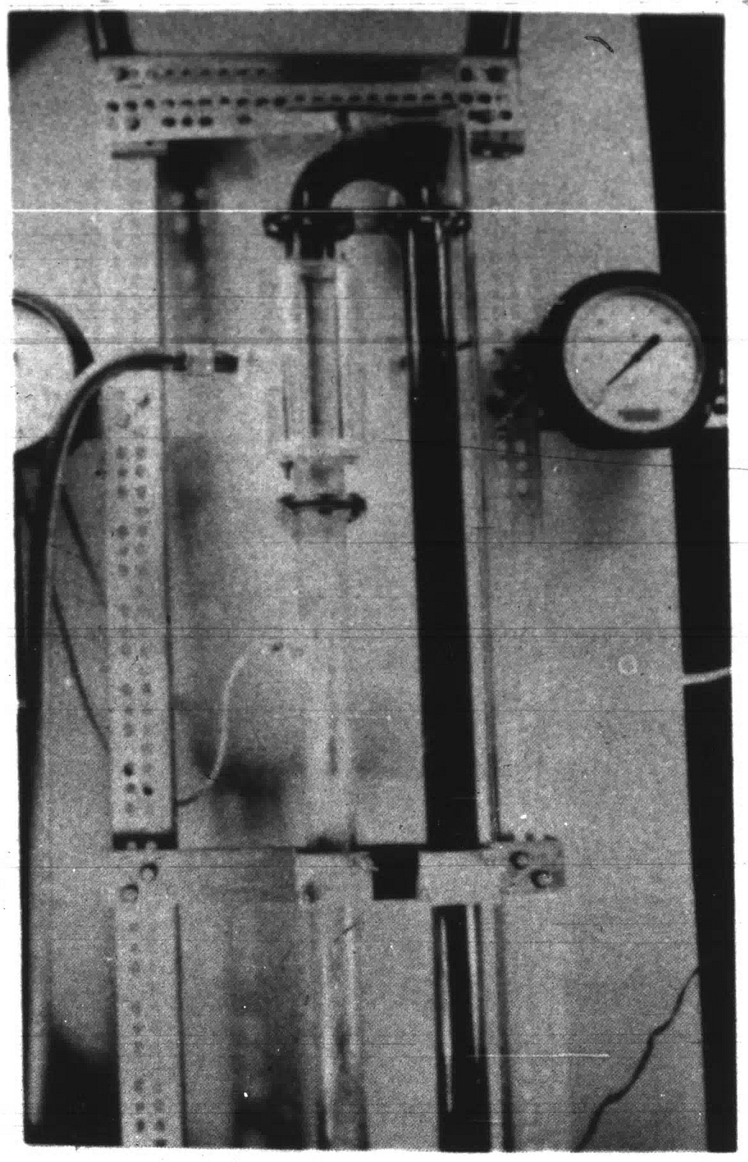

F.V.P.-A.B.2-W.15

Fig. 35.

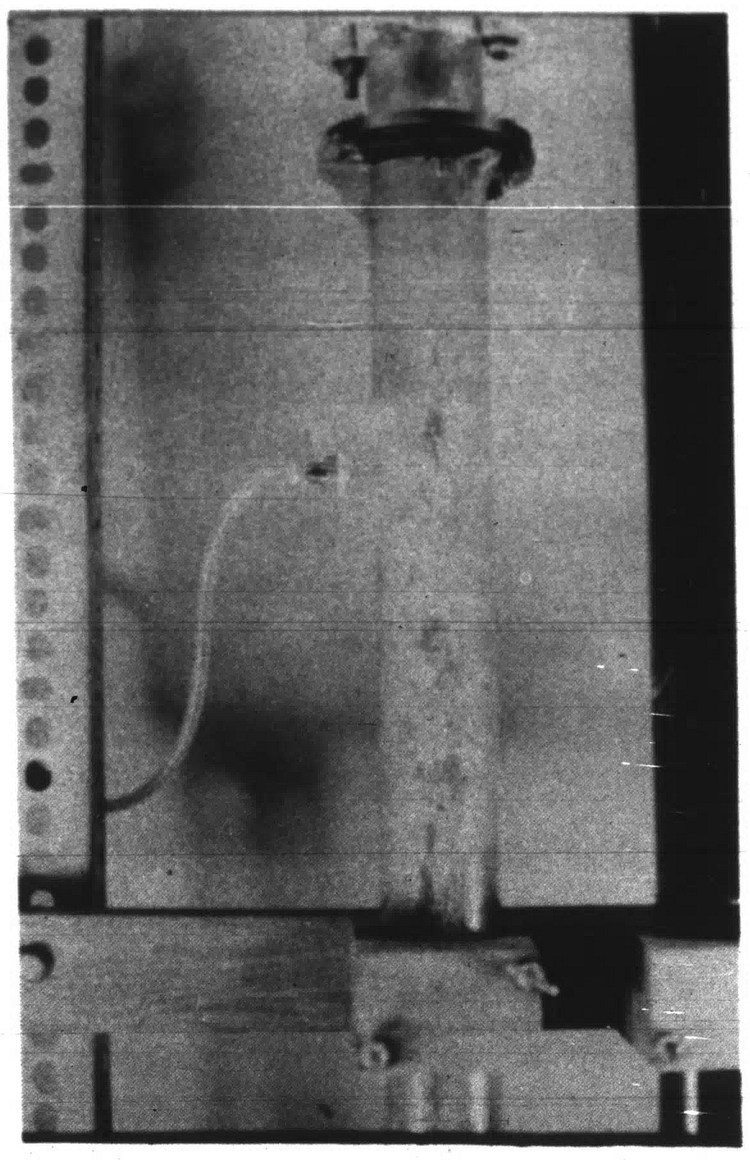

C.V.P.-A.B.2-W.15

Fig. 36.

Fig. 33-36.

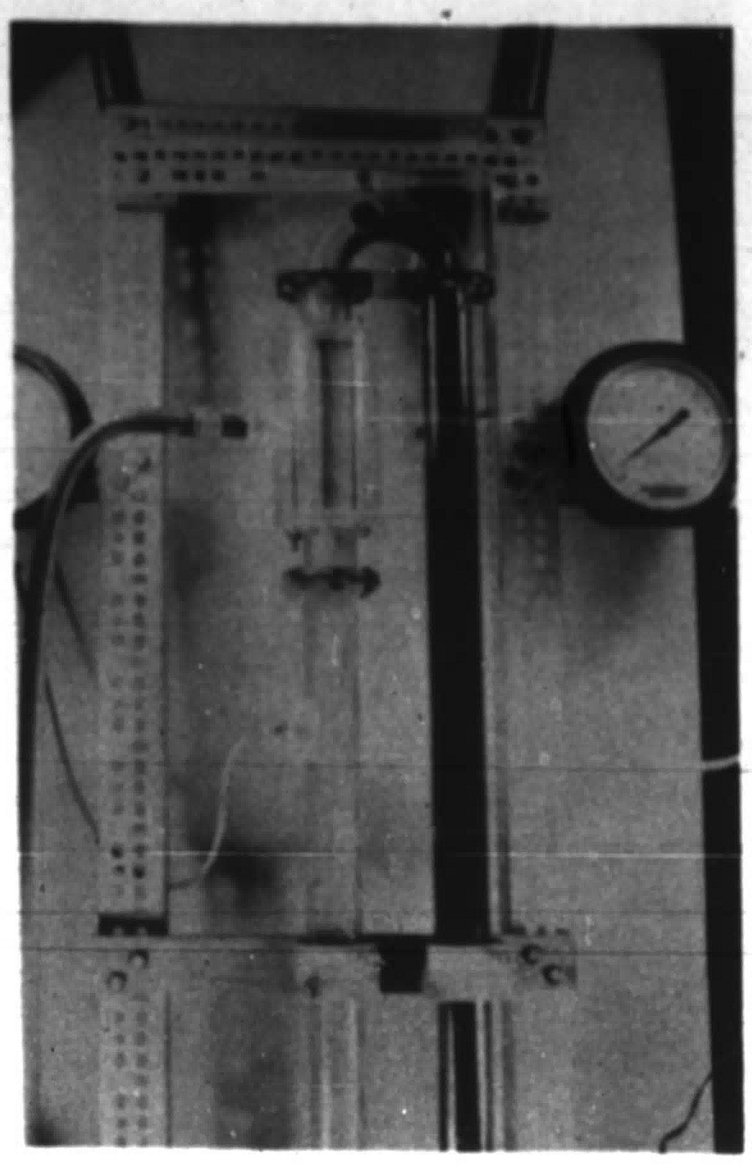

F.V.P.-A.B..25-W.3

Fig. 37.

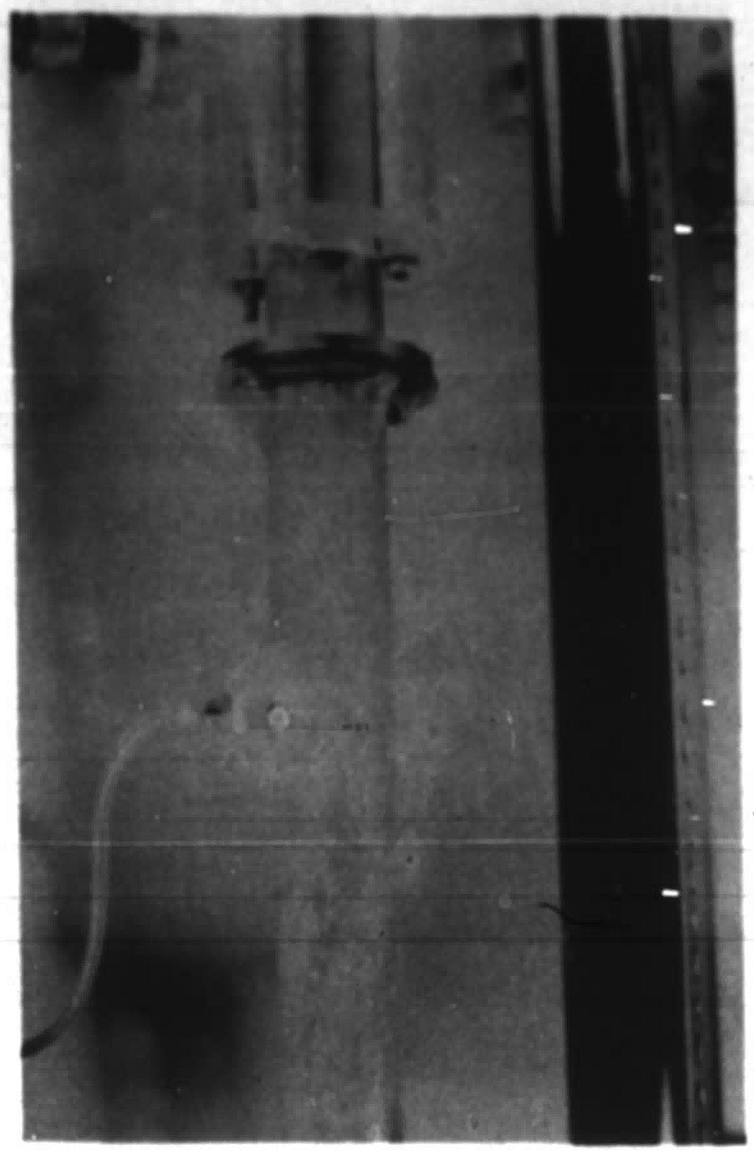

C.V.P.-A.B..25-W.3

Fig. 38.

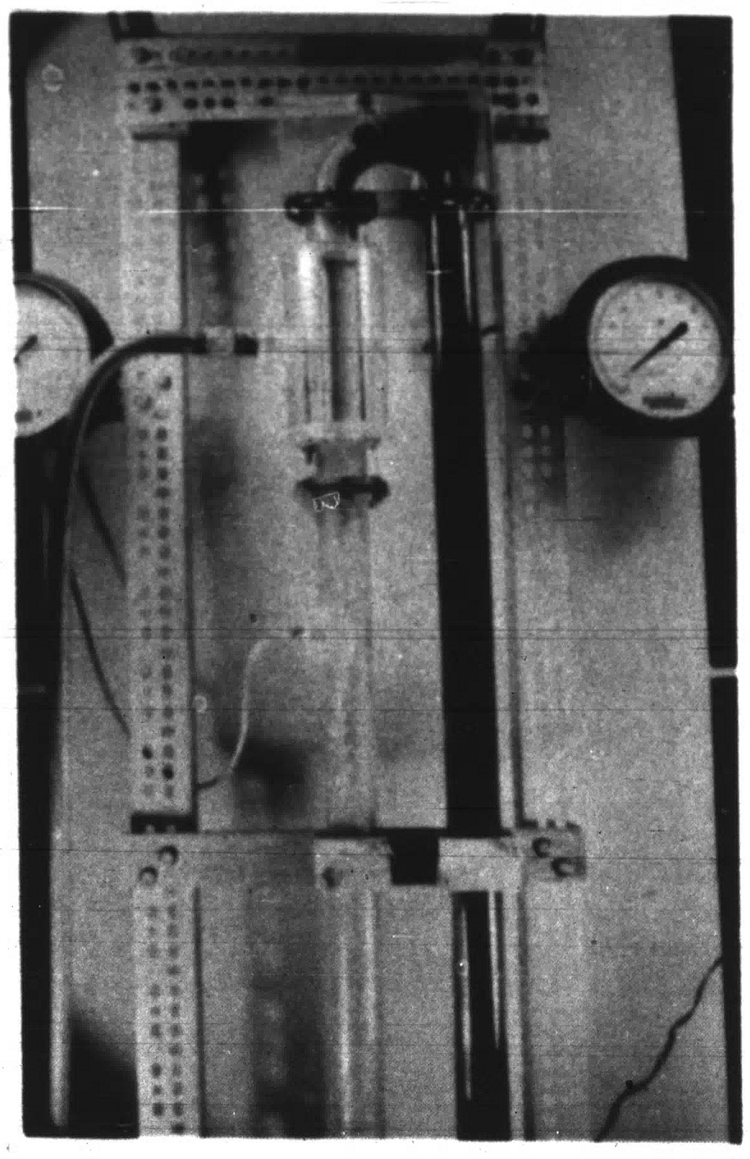

F.V.P.-A.B..25-W.4

Fig. 39.

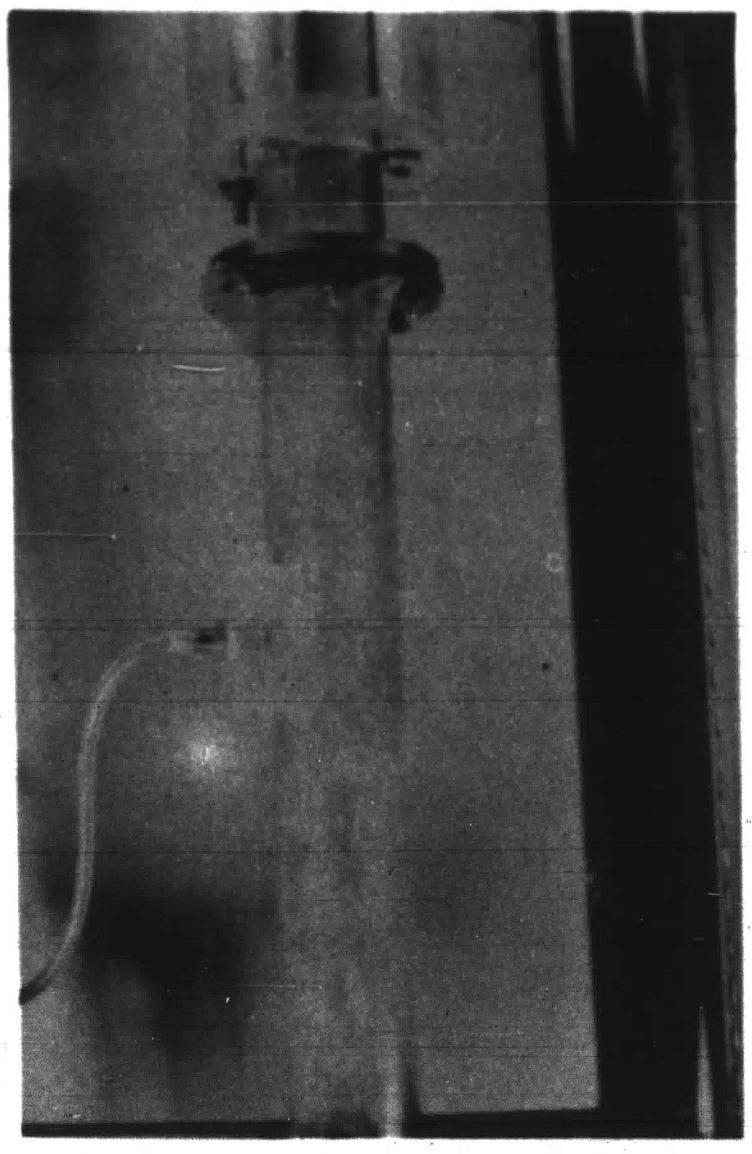

C.V.P.-A.B..25-W.4

Fig. 40.

Fig. 37-40.

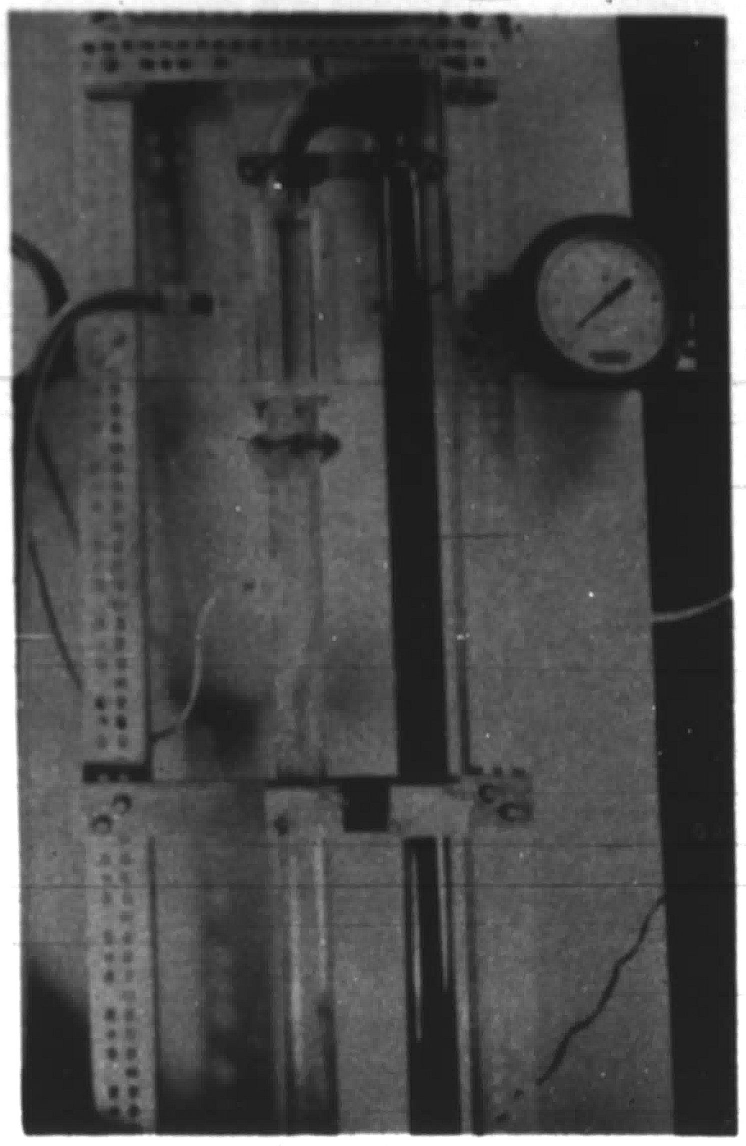

F.V.P.-A.B..25-W.5

Fig. 41.

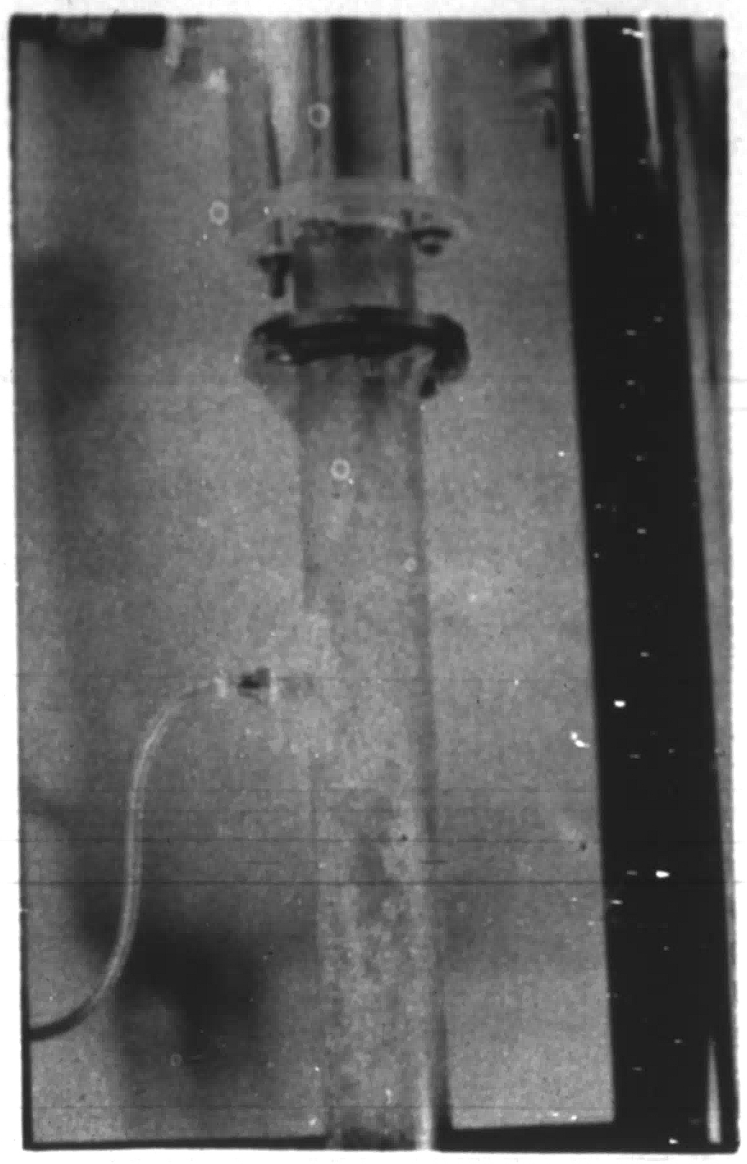

C.V.P.-A.B..25-W.5

Fig. 42.

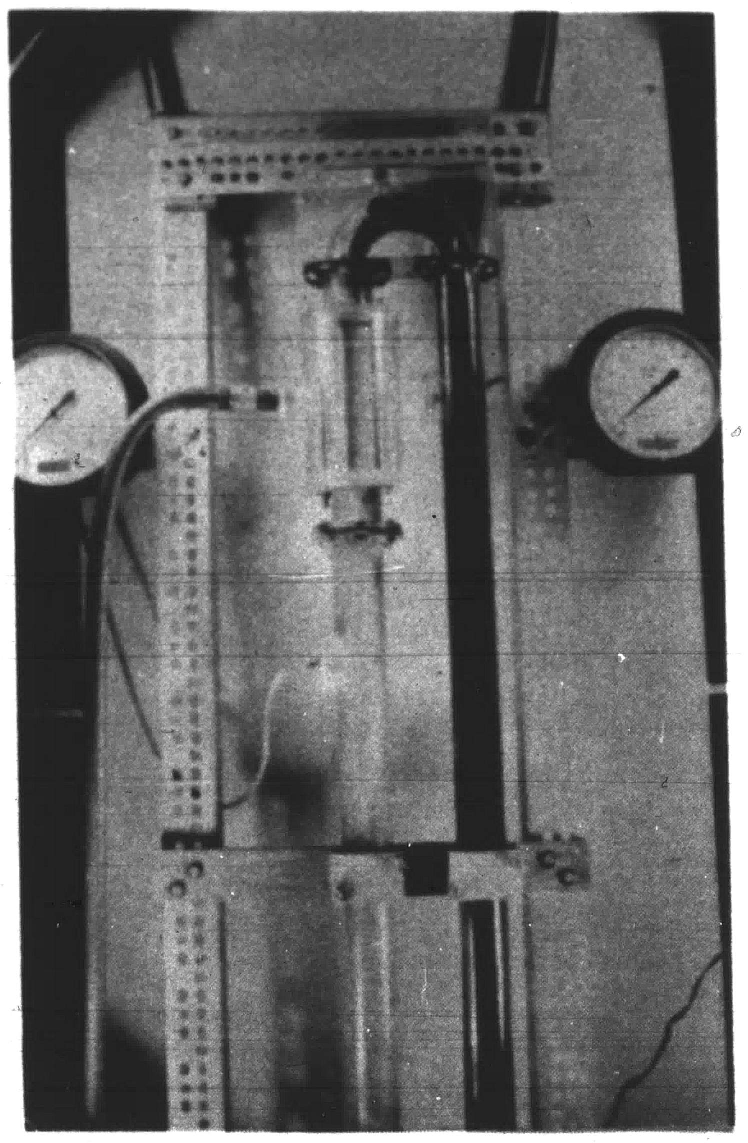

F.V.P.-A.B..25-W.6

Fig. 43.

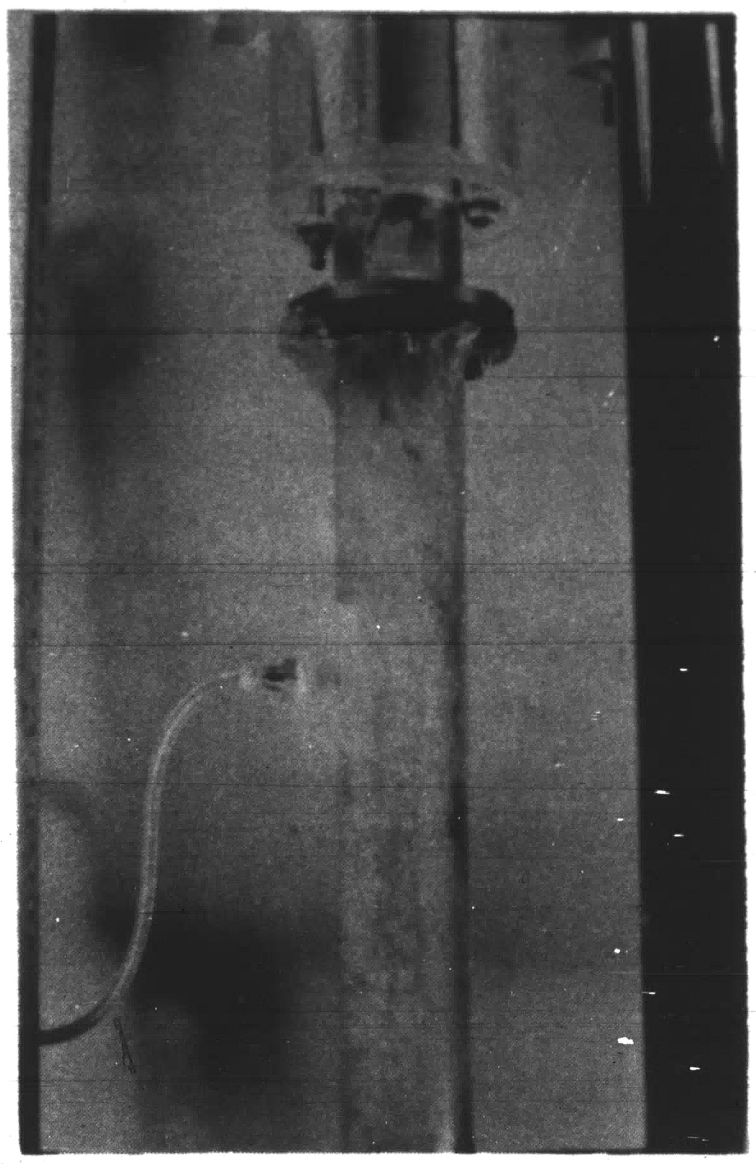

C.V.P.-A.B..25-W.6

Fig. 44.

Fig. 41-44.

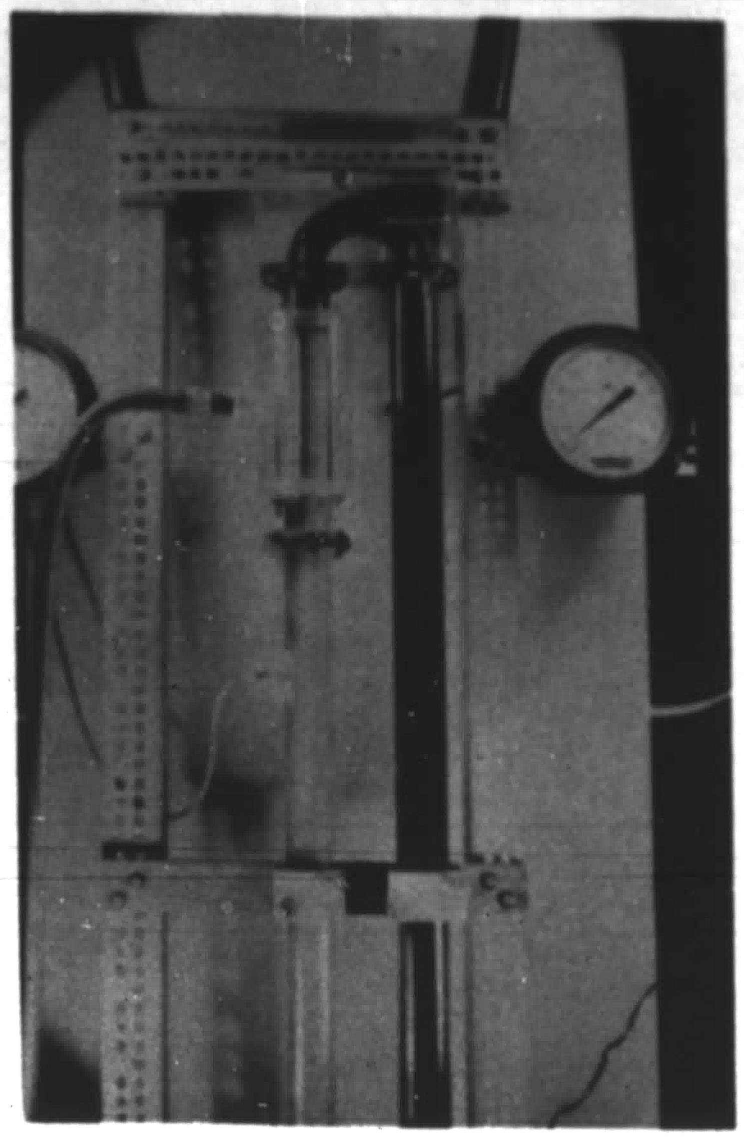

F.V.P.-A.B..25-W.6.8

Fig. 45.

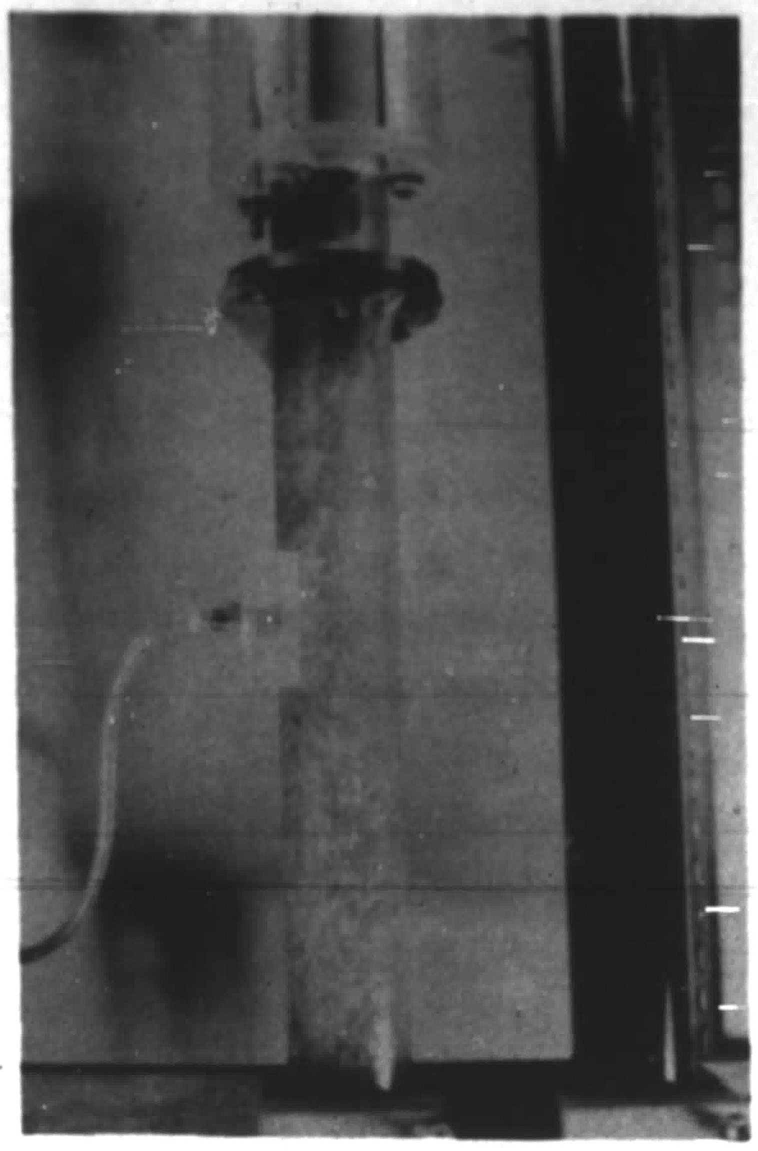

C.V.P.-A.B..25-W.6.8

Fig. 46.

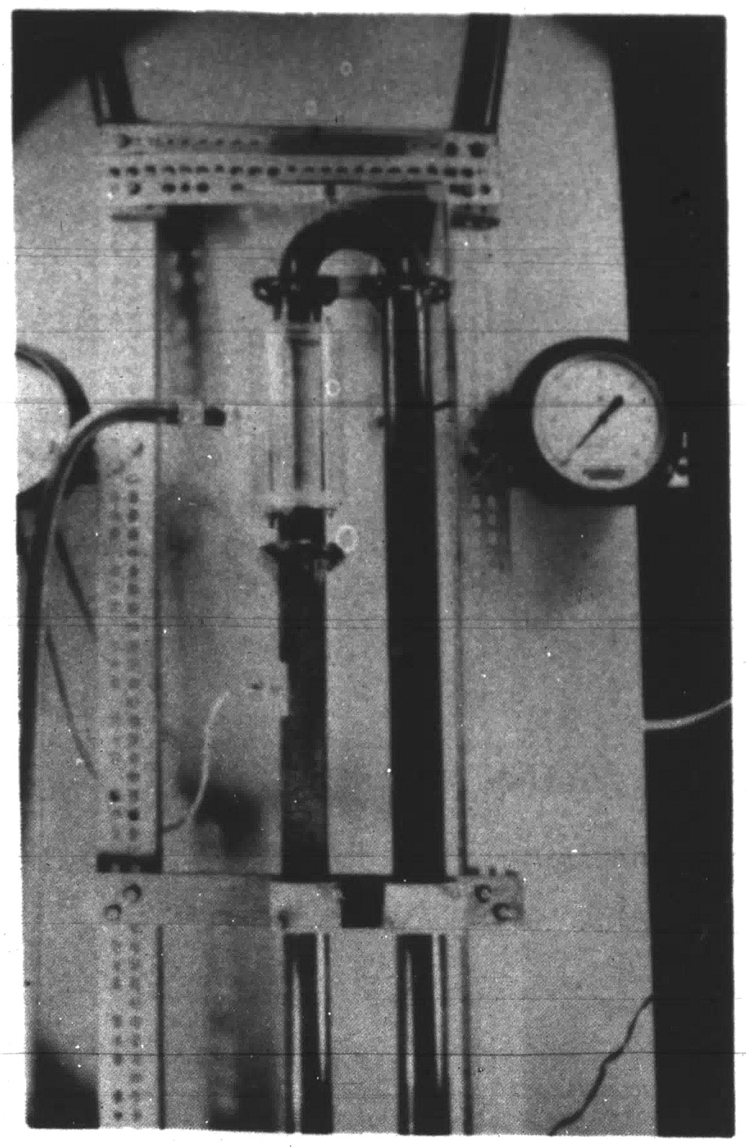

F.V.P.-A.B..25-W.7

Fig. 47.

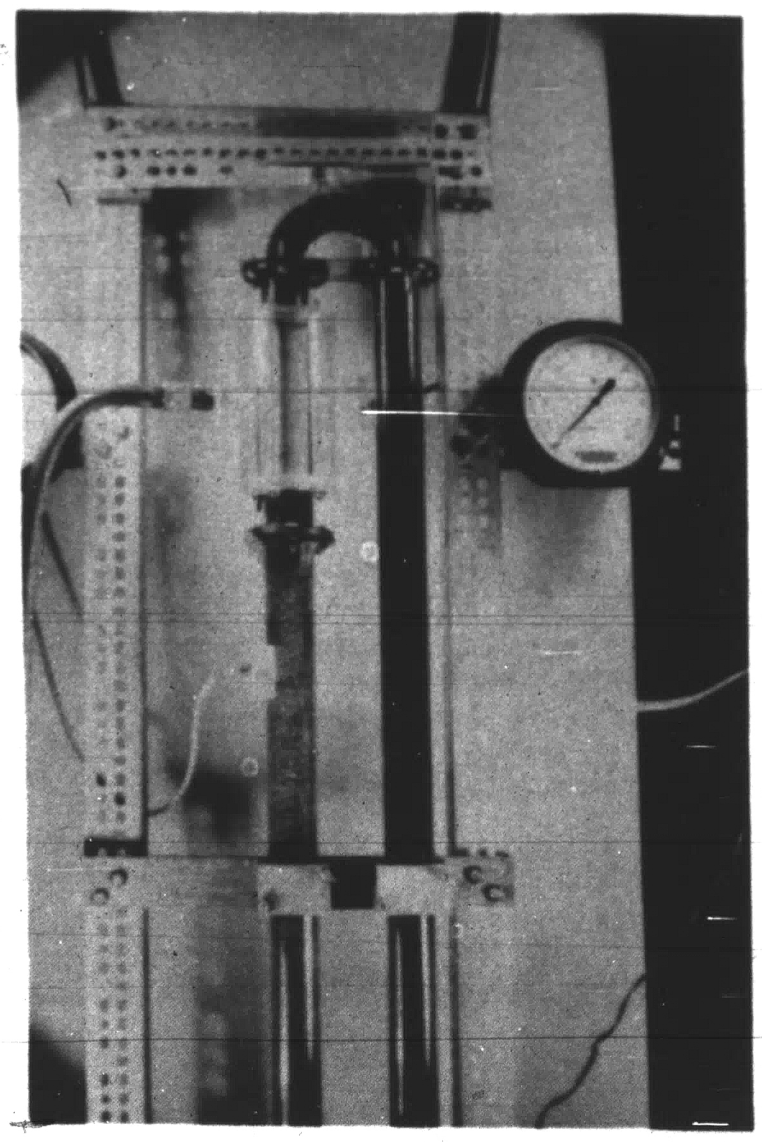

F.V.P.-A.B..25-W.8

Fig. 48.

Fig. 45-48.

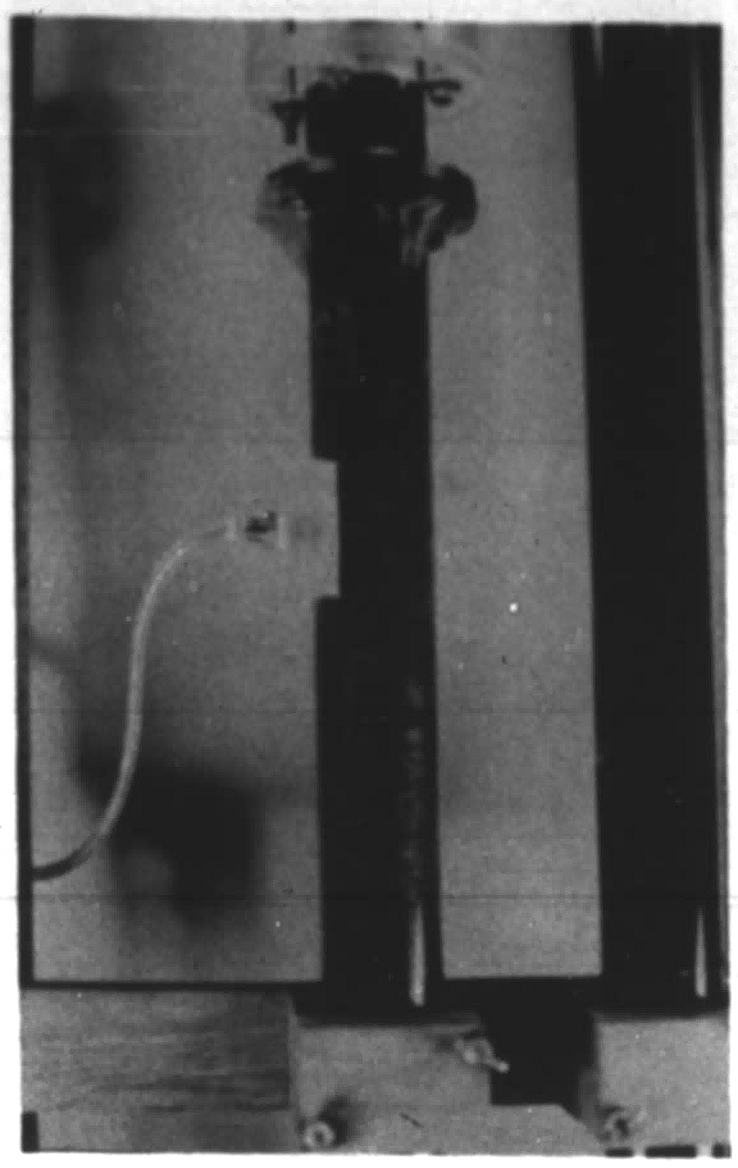

C.V.P.-A.B..25-W.8

Fig. 49.

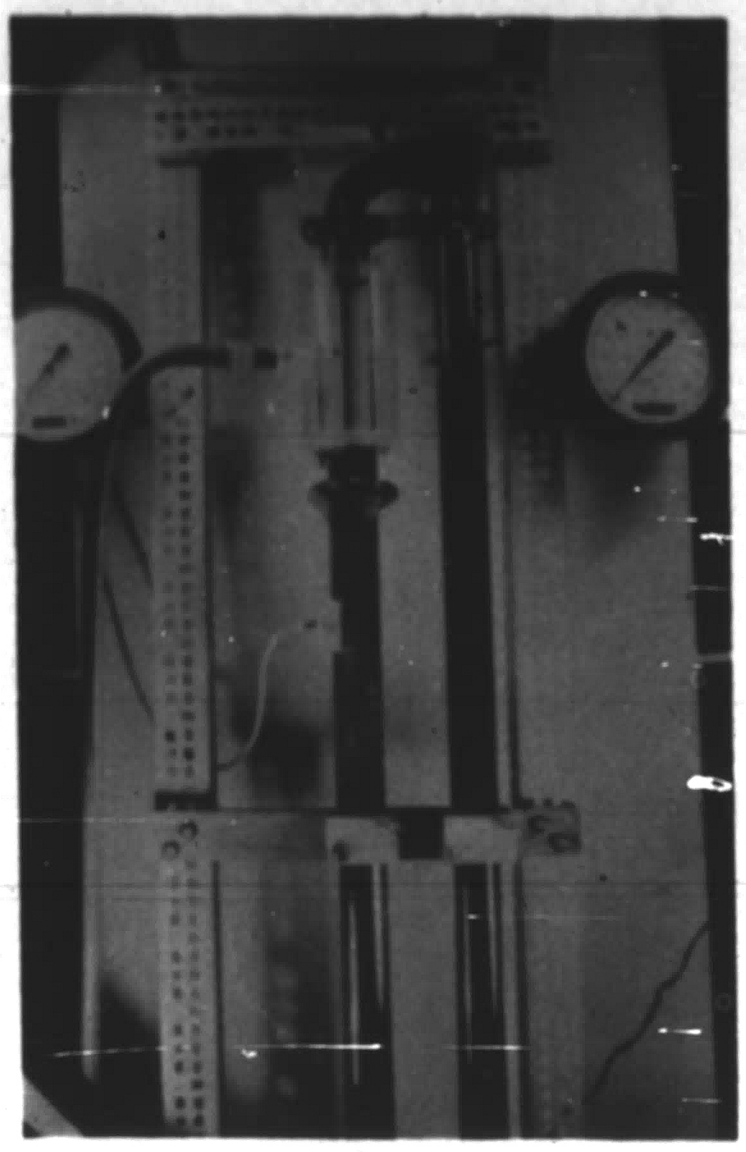

F.V.P.-A.B..25-W.10

Fig. 50.

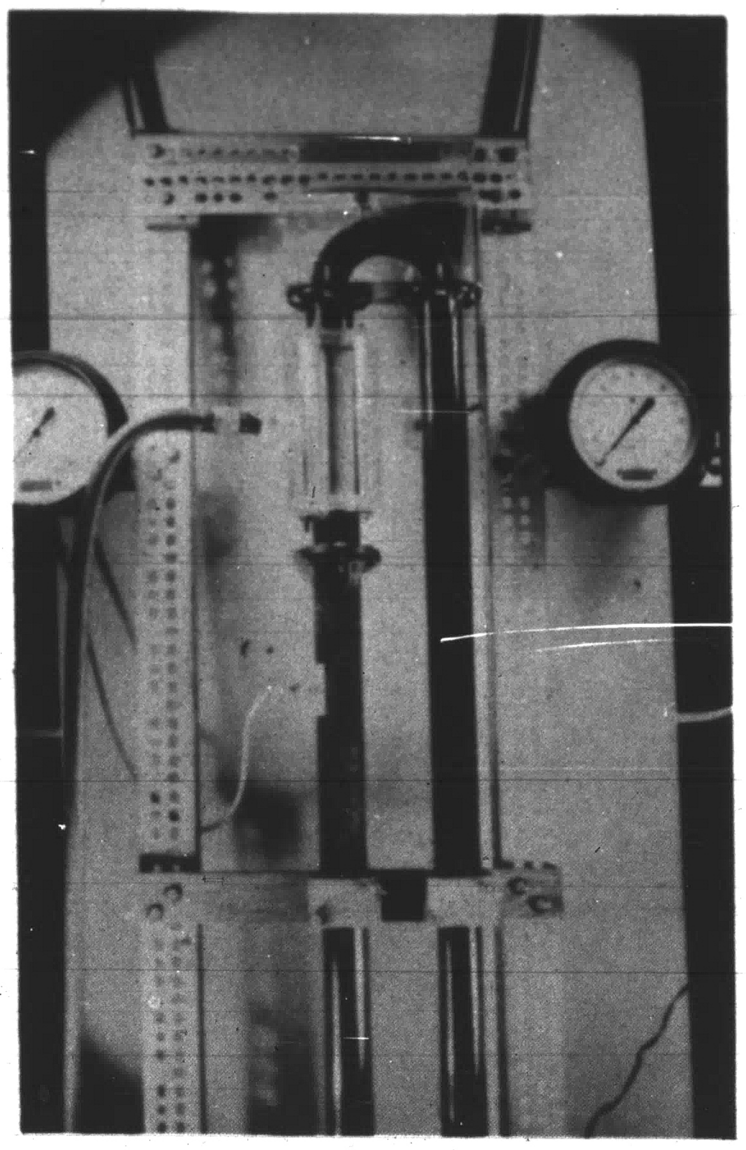

F.V.P.-A.B..25-W.15

Fig. 51.

Fig. 49-51

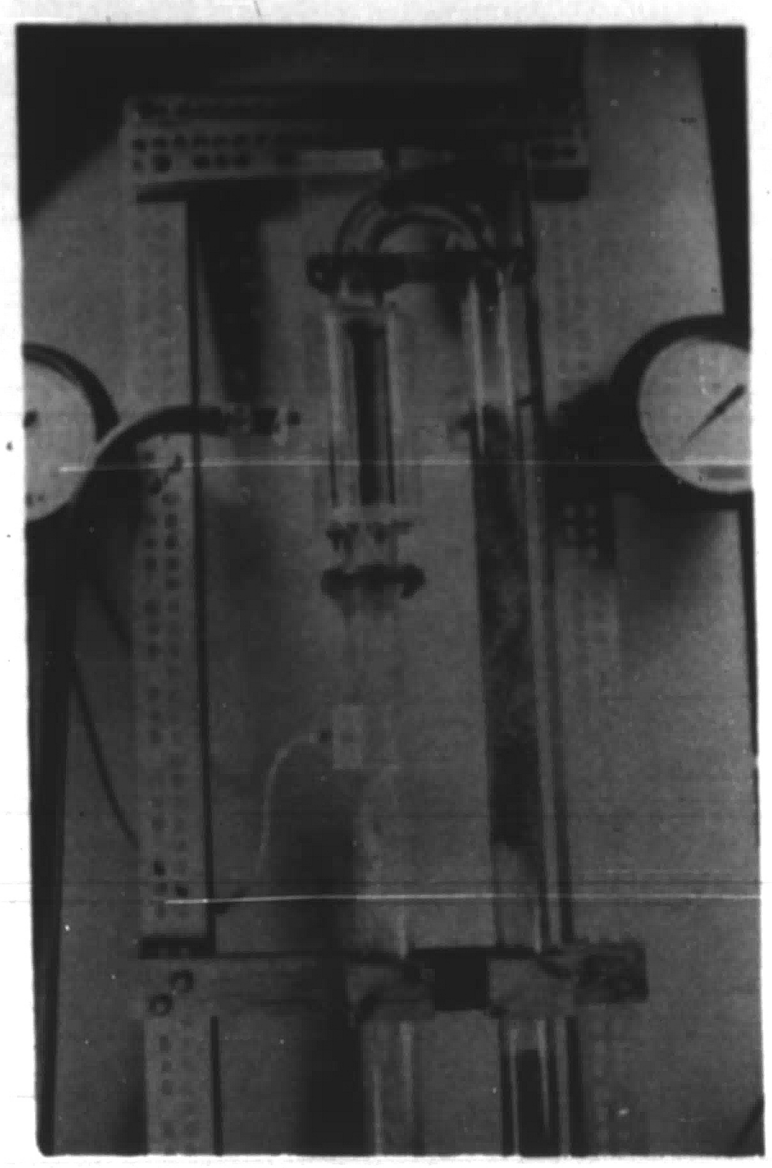

F.V.P.-A.I.2-A.B.2-W.3

Fig. 52.

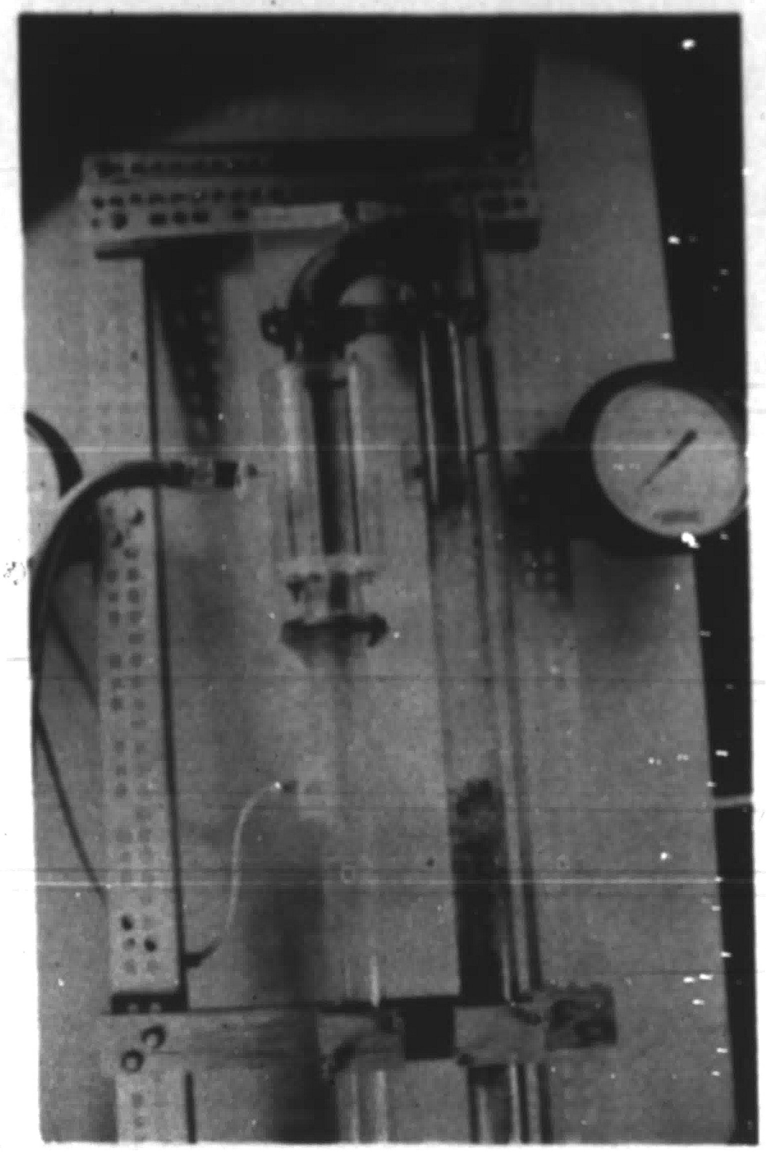

F.V.P.-A.I.2-A.B.2-W.3

Fig. 53.

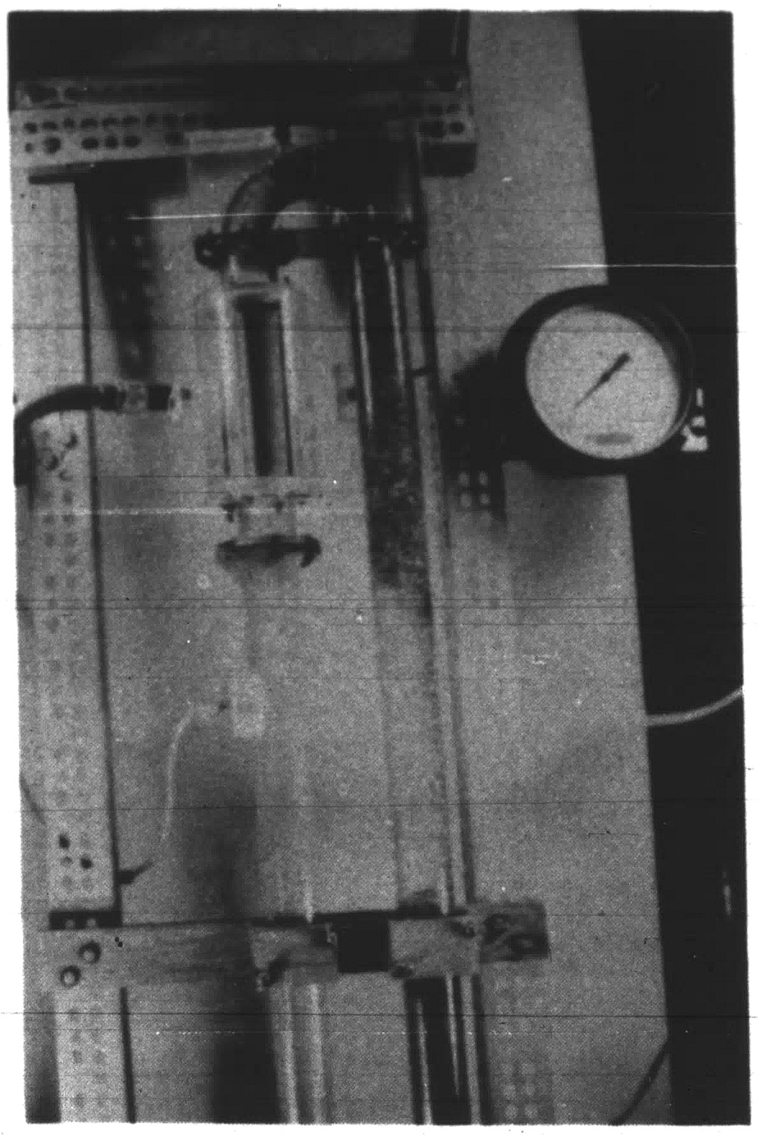

F.V.P.-A.I.2-A.B.2-W.3

Fig. 54.

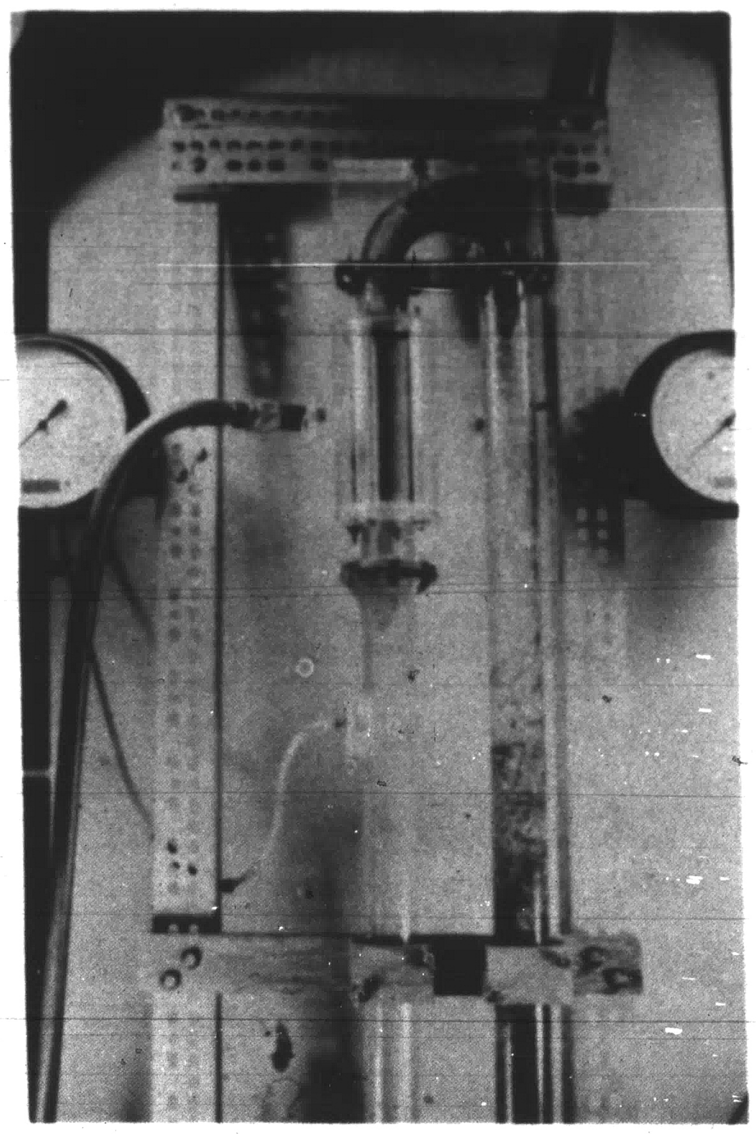

F.V.P.-A.I.2-A.B.2-W.1.5

Fig. 55

Fig. 52-55.

REFERENCES

1. Luis Pujol, "Boiling heat transfer in vertical upflow and downflow tubes", Ph.D. Dissertation Lehigh University, June 1968.

2. L. P. Golan, "An air-water study of vertical upward and downward two-phase flow", Ph.D. Dissertation Lehigh University, 1968.

3. L. S. Tong, "Boiling heat transfer and two phase flow", 1965 - John Wiley and Sons, Inc.

4. Peter Griffith, "Two phase flow in pipes". Developments in heat transfer M.I.T. press (1964), pp. 261-292.

VITA

Chandrakant Vishwanath Mahale alias Hari was born in Ankola, India, on July 15, 1943. He is the third son of Vishwanath and Bhagirathi Mahale. Mr. Mahale did his high school education at C. L. Boy's High School in Bombay, India, completed First Year Science and Intermediate Science at D. G. Ruparel College, Bombay and received his Bachelor of Electrical Engineering and Bachelor of Mechanical Engineering from Walchand College of Engineering in October, 1965 and 1967 respectively.

He worked as a Tutor Demonstrator in Victoria Jubilee Technical Institute, Bombay. Previous to this appointment he worked as a Sectional Officer (supervision) at Bandra Electric Sub Division, Bombay.

Mr. Mahale held the R. D. Sethna Scholarship for higher studies. He came to Lehigh University in the spring semester of 1968.